




## Article

# Evaluating the Performance of Synthetic Double Sampling $np$ Chart Based on Expected Median Run Length

Moi Hua Tuh <sup>1,2,\*</sup> , Cynthia Mui Lian Kon <sup>2</sup>, Hong Siang Chua <sup>2</sup>, Man Fai Lau <sup>3</sup>  and Yee Hui Robin Chang <sup>4</sup> 

- <sup>1</sup> Faculty of Computer and Mathematical Sciences, Universiti Teknologi MARA, Cawangan Sarawak, Kota Samarahan 94300, Sarawak, Malaysia
- <sup>2</sup> Faculty of Engineering, Computing and Science, Swinburne University of Technology Sarawak Campus, Kuching 93350, Sarawak, Malaysia
- <sup>3</sup> School of Software and Electrical Engineering, Swinburne University of Technology, Melbourne, VIC 3122, Australia
- <sup>4</sup> Faculty of Applied Sciences, Universiti Teknologi MARA, Cawangan Sarawak, Kota Samarahan 94300, Sarawak, Malaysia
- \* Correspondence: [tuhmoihua@uitm.edu.my](mailto:tuhmoihua@uitm.edu.my)

**Abstract:** To keep an eye on the status of high-quality processes for fraction nonconforming, the synthetic double sampling (SDS)  $np$  chart is a helpful tool. The SDS  $np$  chart is a hybrid between the double sampling (DS)  $np$  chart and the conforming run length (CRL) chart. The performance of a control chart is typically judged solely using the average run length (ARL). However, as the shape of the run length (RL) distribution varies with the magnitude of the shift in the process fraction nonconforming, the ARL no longer provides clear interpretation of a chart's performance. Subsequently, enhanced DS  $np$  charts that use median run length (MRL) and expected median run length (EMRL) measures, including SDS  $np$  with MRL have recently been proposed for addressing this setback. To broaden the functionality of SDS  $np$ , in this work, the unexplored use of EMRL as alternative performance measure is developed by means of Markov chain model. Additionally, in both the zero-state (ZS) and steady-state (SS) modes, the novel optimal designs algorithms are described for computing the optimal charting parameters of the SDS  $np$  chart, for both MRL<sub>1</sub> and EMRL<sub>1</sub> minimizations, without any unfavourable feature of bilateral sensitivity. Both the MRL and EMRL performances of SDS  $np$ , synthetic  $np$ , and DS  $np$  charts are compared. Optimal designs charting parameters and sensitivity analyses are provided to aid the practical application of SDS  $np$  chart.

**Keywords:** Markov chain; median run length; unknown shift size; zero-state; steady-state; synthetic  $np$

**MSC:** 49M37



**Citation:** Tuh, M.H.; Kon, C.M.L.; Chua, H.S.; Lau, M.F.; Chang, Y.H.R. Evaluating the Performance of Synthetic Double Sampling  $np$  Chart Based on Expected Median Run Length. *Mathematics* **2023**, *11*, 595. <https://doi.org/10.3390/math11030595>

Academic Editor: Alexander Zeifman

Received: 22 December 2022

Revised: 18 January 2023

Accepted: 20 January 2023

Published: 23 January 2023



**Copyright:** © 2023 by the authors. Licensee MDPI, Basel, Switzerland. This article is an open access article distributed under the terms and conditions of the Creative Commons Attribution (CC BY) license (<https://creativecommons.org/licenses/by/4.0/>).

## 1. Introduction

The Shewhart charts, developed by Walter A. Shewhart in the 1920s, are widely used to identify special causes of a process's variation. Shewhart  $np$  charts have the advantage of being simple to use and comprehend, but they are not sensitive enough to pick up on small and moderate changes in the process fraction nonconforming ( $p$ ). As a result, a number of alternatives to the traditional Shewhart  $np$  chart have been taken into consideration, with the main goal of improving the charts' sensitivity. One alternative that aims to improve upon the traditional Shewhart  $np$  chart is the synthetic double sampling (SDS) scheme.

SDS control charts are generally considered as an efficient process monitoring tool because of their exceptional qualities, such as the capacity to detect tiny and moderate process shifts easily even with a small sample size (see examples [1,2]). Very few researchers, up until this point, have expressed interest in designing SDS charts. An SDS scheme which

combines the double sampling (DS)  $\bar{X}$  and conforming run length (CRL) sub-charts was proposed by Khoo et al. [1] for monitoring the process mean. The latter was introduced by Bourke [3] for the purpose of detecting the process fraction nonconforming  $p$  shifts. The random variable CRL denotes the number of examined sample points which can be found between two consecutive nonconforming sample points, involving the end nonconforming sample point. They demonstrated that in comparison to the exponential weighted moving average (EWMA), synthetic and DS schemes, the SDS is more sensitive to process shifts. Motivated by Khoo et al. [1], Khoo et al. [2] developed a multivariate SDS  $T^2$  chart using the Hotelling  $T^2$  statistic. A SDS  $s$  chart is suggested by Lee and Khoo [4] to track increases in the process standard deviation. Costa and Machado [5] used Markov chain method to investigate the SS properties of standard SDS and side-sensitive SDS  $\bar{X}$  charts. The SDS chart outperforms the DS chart in terms of steady-state (SS) ARL. In addition, their investigation revealed that the side-sensitive rule enhances the overall performance of the SDS  $\bar{X}$  chart, but not enough to surpass the performance of the standard DS  $\bar{X}$  chart. Using information on auxiliary characteristics, Haq and Khoo [6] proposed an auxiliary information-based (AIB) SDS chart for the process mean by combining the CRL chart with the existing AIB double sampling (AIB DS) chart. You et al. [7] extended the work of the SDS  $\bar{X}$  chart with known process parameters proposed by Khoo et al. [1] to the estimated process parameters case. They investigated the performance of the SDS  $\bar{X}$  chart with estimated process parameters, in terms of the average run length (ARL), average number of observations to signal (ANOS) and standard deviation of the run length (SDRL). You [8] looked into the performance of the SDS chart developed by You et al. [7] with known and estimated process parameters using the expected average run length (EARL). This study has shown that the performance criterion EARL can tackle the unknown shift size problem. By adopting the cost model from Lorenzen and Vance [9], Lee and Khoo [10,11] explored the economic and economic statistical designs for the SDS  $T^2$  and SDS  $\bar{X}$  charts, correspondingly. In terms of economic performance, the numerical comparison shows that the SDS chart is superior to the competing charts. Aghaulor and Ezekwem [12] proposed an economic design approach to estimate the parameters of the SDS control chart and DS  $\bar{X}$  control chart.

For the attribute type control chart, Chong et al. [13] proposed a SDS  $np$  chart for detecting increases in the fraction of nonconforming items. They demonstrated that the zero-state (ZS) ARL performance of the SDS  $np$  chart outperforms the competing charts. Following Chong et al. [13], Tuh et al. [14] subsequently studied the SDS  $np$  chart based on MRL. Their work provides us with the opportunity to continue expanding the suitability of the SDS  $np$  chart in the field of attribute data in SPC. There have been earlier reports [15] suggesting not to implement the synthetic scheme since its monitoring effectiveness is only confined to specific change conditions, often in cases in which the occurrence of change is at the start of monitoring. Nevertheless, subsequent work by Malela-Majika [16] rebuffed the negativity surrounding this scheme, concluding that the use of the synthetic scheme with fit optimal parameters remains appropriate and highly sensitive to process shift, particularly under large lower limit of the CRL sub-chart.

It is demonstrated that the zero-state (ZS) and steady-state (SS) modes of the run length (RL) distribution of the synthetic chart are shown to be very different [17,18]. In the ZS mode, it is assumed that the change in the process parameter(s) occurred during the start of monitoring, so that there is a nonconforming sample at time zero. In this way, an out-of-control (OOC) signal will be generated if there is a second nonconforming sample within the next  $H$  samples (i.e., when the  $CRL \leq H$ ), where  $H$  is a specified positive integer. This, according to Davis and Woodall [17], gives the synthetic chart an advantage over other popular charts because of this head-start features. It is crucial to evaluate the SS performance of the synthetic chart [17,18], as its detection of delayed shifts may be slower since the effect of the head-start is lost.

The average run length (ARL)'s lone use as the performance measure for control charts was questioned by numerous researchers. For example, see Teoh et al. [19], Khoo et al. [20],

Lee and Khoo [21]. In addition, as pointed out by Graham et al. [22], utilizing the ARL as a performance measure has a number of disadvantages and may overlook some vital statistical properties of control charts. The RL is a positive integer random variable, and it is noted that the RL distribution changes from being significantly right skewed when the process shift is small to being almost symmetric when the process shift is large. In descriptive statistics, the choice of summary measures to describe a distribution is an important aspect. It is well known that when a distribution is right skewed, the mean is larger than the median and hence, it is not a fair representation of a “centre”. In this regard, the median is a better measure of “central tendency” and thus, the median run length (MRL) can provide more meaningful information [23].

The MRL is the 50th percentile of the RL distribution. As commented by Chakraborti [23], a Shewhart  $\bar{X}$  chart with  $\pm 3$  standard deviation width has an IC ARL ( $ARL_0$ ) of 370 but 50% of all the run lengths are less than 257 (i.e., the IC MRL ( $MRL_0$ ) is 257) and about 60–70% of all the run lengths are less than 370. The MRL comes in two types, namely in-control (IC) MRL ( $MRL_0$ ) and OOC MRL ( $MRL_1$ ). When  $MRL_0$  is 215, most practitioners will suggest that a control chart certainly detects a false alarm at the 215th sample 50% of the time. This will strengthen practitioners’ confidence when dealing with a few short runs with no assignable causes. When comparing various control charts, to ensure a fair comparison, the  $MRL_0$  value is kept at the same value to provide a fair comparison; the one with the smallest  $MRL_1$  value outperforms the others. The reason for this is that the lower the  $MRL_1$ , the faster the shift is observed.

In order to compute the MRL, practitioners need to specify the process shift size in advance. However, quality practitioners are typically unaware of the process shift size. Due to relatively scarce practice-based historical data, quantifying the amount of process transformation is a hard challenge for practitioners. Aside from that, the shift size fluctuates based on unidentified random occurrences. Moreover, if a practitioner considers a certain shift size and utilises its optimal charting parameters, the control chart will perform poorly when a different shift size actually happens. In order to overcome these issues, it is necessary to adopt the expected median run length (EMRL) as an alternative performance measure, which requires simply a range of process shift sizes. Among others, Teoh et al. [24], Tang et al. [25], Qiao et al. [26], Chong et al. [27] and Tuh et al. [28] considered the EMRL performance criterion in their recent studies.

The primary objective of this work is, therefore, to extend the contributions of Tuh et al. [14,28] by employing EMRL as the performance measure in developing the SDS  $np$  chart. In this work, both ZS and SS performance evaluations are considered for the charts being studied. This work provides the optimal chart’s design procedures for the SDS  $np$  chart based on  $MRL_1$  and  $EMRL_1$  minimizations (for known and unknown shift sizes cases). For this purpose, the model developed by Tuh et al. [14], which focusses on the optimal charting parameter SDS  $np$  when  $MRL_{0min}$  of 200, is adopted herein for hitherto unexplored  $MRL_{0min}$  of 370.4, as a mean to make performance comparison with the competing charts. As envisioned, for zero-state mode, the SDS  $np$  chart possesses both the power of the synthetic chart for rapidly detecting moderate and minor shifts and the advantage of the DS  $np$  chart for sensitivity to significant shifts, resulting in a superior and more uniform overall performance. The subsequent sections of this article are organised as follows: A description of the plotting statistic and certain characteristics of the SDS  $np$  chart is presented in Section 2. Following a discussion of the RL distribution properties of the SDS  $np$  chart in Section 3, Section 4 describes the optimization designs of the proposed SDS  $np$  chart, in both ZS and SS mode, using MRL and EMRL performance criteria. In Section 5, the effectiveness of the synthetic  $np$ , DS  $np$ , and SDS  $np$  charts in both known and unknown shift size situations are compared. Section 6 provides an illustration of the implementation of the EMRL-based optimal SDS  $np$  chart by including a process that produces ballpoint pen cartridges. In the final section, conclusions are drawn.

## 2. The Review of SDS $np$ Chart

The SDS  $np$  chart proposed by Chong et al. [13], is an integration of the DS  $np$  and CRL sub-charts. The CRL stands for the number of examined sampling stages ( $i$ ) between two consecutive nonconforming sampling stages (taking into account the nonconforming sampling stages at the end). The elements from the two sub-charts are included in the design of the SDS  $np$  chart. They are (i) the lower limit  $H$  of the CRL sub-chart, and (ii) the DS  $np$  sub-chart element that encompasses the initial sample size  $n_1$ , second sample size  $n_2$ , the first stage warning limit  $W$ , first stage control limit  $L_1$  and the second stage control limit  $L_2$ . It should be noted that  $H$  is a positive integer.

The trio of non-integer control limits  $W$ ,  $L_1$  and  $L_2$  of the DS  $np$  sub-chart are established as  $W = Ac_1 + 0.5$ ,  $L_1 = Re_1 - 0.5$  and  $L_2 = Ac_2 + 0.5$  (also described in [13,29,30]) to eliminate uncertainty among quality professionals, particularly when the observed quantity of nonconforming items exceeds the control limits.

The IC and OOC processes on the DS  $np$  chart are classified as the conforming and nonconforming sampling stages, respectively, on the DS  $np$  sub-chart component of the SDS  $np$  chart, as shown in Figure 1. The classification of a sampling stage as either conforming or nonconforming depends on the information about the quality characteristic given by the first sample alone or the combined information contained in the first and second samples.

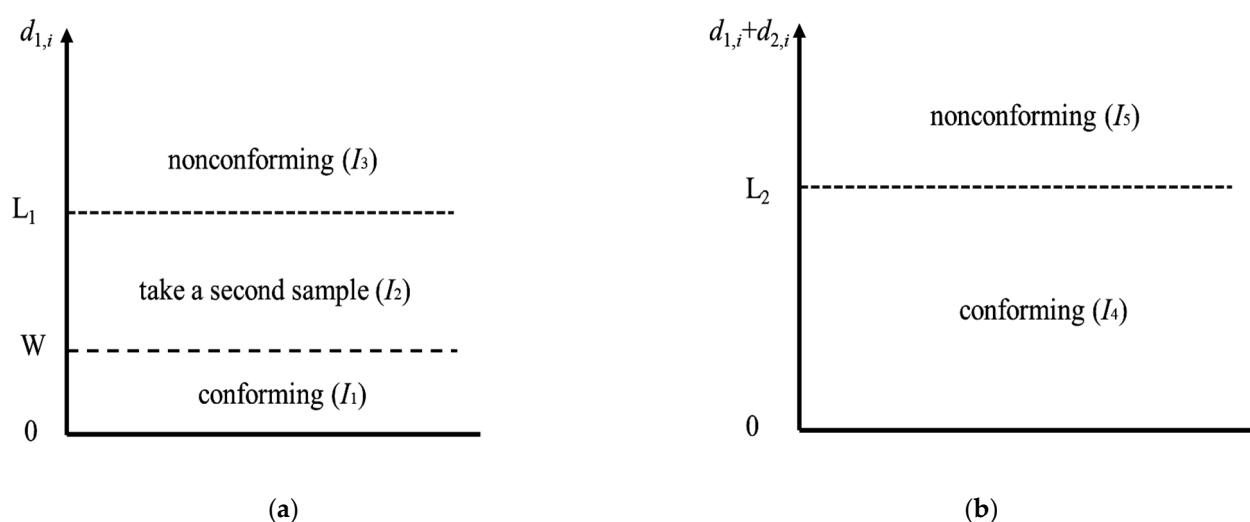


**Figure 1.** Graphical view at (a) first stage and (b) second stage of the DS sub-chart's operation.

The DS  $np$  sub-chart is constructed by first identifying a sampling stage as either conforming or nonconforming based on the process information provided by the first sample or the combined first and second samples. The CRL sub-chart is necessary for determining whether or not the sample is OOC. The following steps are a description of how the SDS  $np$  chart operates:

- Step 1: Set the optimal charting parameters  $W$ ,  $L_1$ ,  $L_2$  (on DS sub-chart) and  $H$  (on CRL sub-chart).
- Step 2: Consider the first sample of size  $n_1$  and count the number of nonconforming items  $d_1$  in the sample.
- Step 3:
  - (i) If  $d_{1,i} \in I_1$ , the  $i$ th sampling stage is categorized as conforming. Process returns to Step 2.
  - (ii) If  $d_{1,i} \in I_3$ , the  $i$ th sampling stage is categorized as nonconforming and control flow advances to Step 5.
  - (iii) If  $d_{1,i} \in I_2$ , the procedure moves to the second stage of the DS sub-chart. A second sample of size  $n_2$  is taken and the number of nonconforming items  $d_2$  in the sample is counted. After that, proceed to the next step.

- Step 4: Compute the number of nonconforming items in combined samples  $d_{1,i} + d_{2,i}$ . If  $(d_{1,i} + d_{2,i}) \in I_4$ , the  $i^{\text{th}}$  sampling stage is categorized as conforming and the control flow returns to Step 2. If this is not the case, the sampling stage is categorized as nonconforming, and the control flow moves to Step 5.
- Step 5: Count the number of sampling stages, including the current nonconforming sampling stage, that separate two successive nonconforming sampling stages and is known as CRL value.
- Step 6: If  $\text{CRL} > H$ , the process is deemed as IC and the control flow goes back to Step 2. Otherwise, the process is judged as OOC and corrective action is required to search and eliminate the assignable cause(s). Then, the process goes back to Step 2.

A nonconforming sample may be present if  $d_{1,i} \in I_3$  or  $(d_{1,i} \in I_2 \text{ and } (d_{1,i} + d_{2,i}) \in I_5)$ . The sample's OOC status can only be determined using the CRL sub-chart. The process is considered as IC if  $\text{CRL} > H$ . If not, the process is deemed OOC, and corrective action is needed to identify and remove the assignable cause(s). The operation of the SDS  $np$  chart is graphically summarized in Figure 2.

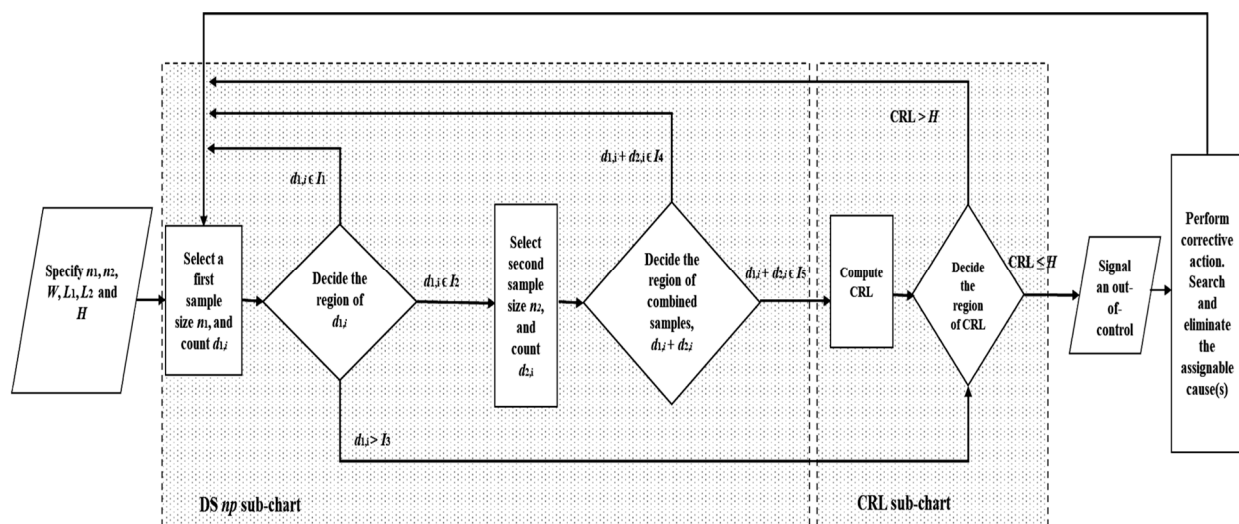


Figure 2. The operational flow chart for the SDS  $np$  chart.

### 3. The Run Length Properties of the SDS $np$ Chart

The Markov chain model provided by Davis and Woodall [17], studied synthetic  $\bar{X}$  chart, is applied to assess RL properties of the SDS  $np$  chart in this work. This approach may be easily expanded to represent the SDS  $np$  chart, allowing for the entire RL distribution of the chart to be obtained.

Let  $A$  denote the probability that a plotted sample statistic of a sampling stage  $i$  falling within the chart limits of the DS  $np$  sub-chart can be expressed as [13]

$$A = A_1 + A_2 \quad (1)$$

where

$$A_1 = P(d_{1,i} \leq [W]) = \sum_{d_{1,i}=0}^{[W]} \frac{n_1!}{d_{1,i}!(n_1 - d_{1,i})!} p^{d_{1,i}} (1-p)^{n_1-d_{1,i}} \quad (2)$$



$$A_2 = P(\lfloor W \rfloor < d_{1,i} < \lceil L_1 \rceil \cap d_{1,i} + d_{2,i} \leq \lfloor L_2 \rfloor)$$

$$= \sum_{d_{1,i}=\lfloor W \rfloor+1}^{\lceil L_1 \rceil-1} \left[ \frac{n_1!}{d_{1,i}!(n_1-d_{1,i})!} p^{d_{1,i}} (1-p)^{n_1-d_{1,i}} \left( \sum_{d_{2,i}=0}^{\lfloor L_2 \rfloor-d_{1,i}} \frac{n_2!}{d_{2,i}!(n_2-d_{2,i})!} p^{d_{2,i}} (1-p)^{n_2-d_{2,i}} \right) \right] \quad (3)$$

The notations  $\lfloor \cdot \rfloor$  and  $\lceil \cdot \rceil$  denote the round down and round up to the nearest integer, respectively. Note that  $A_1$  is the probability that  $d_{1,i} < W$  at the first stage of the DS sub-chart, while  $A_2$  is the probability that  $W < d_{1,i} < L_1$  at the first stage of the DS sub-chart and  $(d_{1,i} + d_{2,i}) < L_2$  at the second stage of the DS sub-chart. Hence,  $B = 1 - A$ .

The partitioned form of the transition probability matrix (TPM)  $\mathbf{P}_{(H+2, H+2)}$  is [20]

$$\mathbf{P} = \begin{pmatrix} \mathbf{R} & \mathbf{r} \\ \mathbf{0}^T & 1 \end{pmatrix} = \begin{pmatrix} A & B & 0 & 0 & \cdots & 0 & 0 \\ 0 & 0 & A & 0 & \cdots & 0 & B \\ 0 & 0 & 0 & A & \cdots & 0 & B \\ \vdots & \vdots & \vdots & \vdots & \ddots & \vdots & \vdots \\ 0 & 0 & 0 & 0 & \cdots & A & B \\ A & 0 & 0 & 0 & \cdots & 0 & B \\ 0 & 0 & 0 & 0 & \cdots & 0 & 1 \end{pmatrix} \quad (4)$$

with  $(H+1)$  transient states and one absorbing state. The matrix of transient probabilities is denoted by the notation  $\mathbf{R}_{(H+1, H+1)}$ , and it is obtained by cutting off the very last row and the very last column of the matrix  $\mathbf{P}$ . The vector  $\mathbf{r}$  meets the condition that  $\mathbf{r} = \mathbf{1} - \mathbf{R} \cdot \mathbf{1}$  (i.e., the row probabilities of  $\mathbf{P}$  must add up to 1), where  $\mathbf{1}_{(H+1, 1)} = (1, 1, \dots, 1)^T$  and  $\mathbf{0}_{(H+1, 1)} = (0, 0, \dots, 0)^T$ .

Let RL represent the run length of the SDS  $np$  chart, which quantifies how many steps the process to reach the absorbing state. Since the RL is known to be a discrete phase-type random variable for the synthetic chart, its value can be expressed as  $\ell = \{1, 2, 3, \dots\}$ . Then, under the ZS mode, the cumulative distribution function (cdf) of the RL random variable is [31]

$$P(\text{RL} \leq \ell) = \mathbf{s}^T (\mathbf{I} - \mathbf{R}^\ell) \mathbf{1} \quad (5)$$

where the column vector  $\mathbf{s}$  denotes stationary probability with  $(H+1)$  elements and a single element of one and zero in another location, and  $\mathbf{I}_{(H+1, H+1)}$  denotes the identity matrix. It should be noted that  $\mathbf{s} = (0, 1, 0, \dots, 0)^T$  [17].

In the case when the process is under SS mode, the cdf of the RL is [20]

$$P(\text{RL} \leq \ell) = \mathbf{s}_c^T (\mathbf{I} - \mathbf{R}^\ell) \mathbf{1} \quad (6)$$

and it can be calculated by substituting  $\mathbf{s}$  (in Equation (5)) with  $\mathbf{s}_c$ . Note that  $\mathbf{s}_c$  is the column vector of cyclical SS probability  $\mathbf{s}_c^T = (\mathbf{1}^T \mathbf{q})^{-1} \mathbf{q}$  [32], and that  $\mathbf{q}$  may be simply solved using  $\mathbf{q} = (\mathbf{G} - \mathbf{R}^T)^{-1} \mathbf{u}$ . In this case, the  $(H+1) \times (H+1)$  matrix  $\mathbf{G}$  and the  $(H+1)$  column vector  $\mathbf{u}$  are

$$\mathbf{G} = \begin{pmatrix} 2 & 1 & 1 & 1 & \cdots & 1 \\ 0 & 1 & 0 & 0 & \cdots & 0 \\ 0 & 0 & 1 & 0 & \cdots & 0 \\ 0 & 0 & 0 & 1 & \ddots & 0 \\ \vdots & \vdots & \vdots & \vdots & \cdots & \vdots \\ 0 & 0 & 0 & 0 & \cdots & 1 \end{pmatrix} \quad (7)$$

and

$$\mathbf{u} = (1 \ 0 \ 0 \ 0 \ \cdots \ 0)^T \quad (8)$$

Let  $\ell_m$  be the 100 $m$ th percentile of the RL distribution, where  $0 < m < 1$ . Then, the  $\ell_m$  of the SDS  $np$  chart can be calculated in such a way that [33]

$$P(RL \leq \ell_m - 1) \leq m \text{ and } P(RL \leq \ell_m) > m \quad (9)$$

The MRL =  $\ell_{0.5}$  for the SDS  $np$ , when  $m = 0.5$ , is therefore defined as

$$P(RL \leq \ell_{0.5} - 1) \leq 0.5 \text{ and } P(RL \leq \ell_{0.5}) > 0.5 \quad (10)$$

Notably, MRL = MRL<sub>0</sub> represents the IC MRL while MRL = MRL<sub>1</sub> denotes the OOC MRL, which may be achieved when  $\gamma = 1$  and  $\gamma > 1$ , respectively.

The speed at which the SDS  $np$  chart can identify an increasing shift in the process fraction nonconforming  $p$  with a magnitude of shift  $\gamma$  equal to  $p_1/p_0$ , where  $p_1 > p_0$ , is a measure of the chart's effectiveness. Note that  $p = p_0$  when  $\gamma$  equal to 1, and  $p = p_1$  when  $\gamma$  greater than 1. Here,  $p_0$  represents the IC fraction nonconforming while  $p_1$  represents the OOC fraction nonconforming.

In addition to the MRL, the ZS and SS ARL of the synthetic  $np$  chart can be computed through [20]

$$ARL_{ZS} = \mathbf{s}^T (\mathbf{I} - \mathbf{R})^{-1} \mathbf{1} \quad (11)$$

and

$$ARL_{SS} = \mathbf{s}_c^T (\mathbf{I} - \mathbf{R})^{-1} \mathbf{1} \quad (12)$$

individually, by means of the Markov chain method. The  $\mathbf{I}$ ,  $\mathbf{R}$ ,  $\mathbf{1}$ ,  $\mathbf{s}$  and  $\mathbf{s}_c$  have all been defined previously. The average sample size (ASS) in each sampling stage of the DS  $np$  sub-chart is expressible via [29]

$$ASS = n_1 + n_2 [P(\lfloor W \rfloor < d_{1,i} < \lceil L_1 \rceil | p)] \quad (13)$$

where  $P(\lfloor W \rfloor < d_{1,i} < \lceil L_1 \rceil | p)$  denotes the probability of taking the second sample of size  $n_2$ . The IC and OOC ARLs (for both ZS and SS) and ASSs are determined using Equations (11)–(13) when  $p = p_0$  and  $p = p_1$ , correspondingly. The notation  $p_0$  denotes the IC fraction of nonconforming items while the notation  $p_1$  represents the OOC fraction of nonconforming items.

The computation of the expected median RL (EMRL), also denoted as  $E(\ell_{0.5})$  when letting  $\alpha = 0.5$ , where a specific value for shift size  $\gamma$  is not required, rather a range of shift sizes is taken into consideration (between minimum and maximum shifts) and can be determined using [34]

$$EMRL = E(\ell_{0.5}) = \int_{\gamma_{\min}}^{\gamma_{\max}} f_{\gamma}(\gamma) MRL(\gamma) d\gamma \quad (14)$$

Note that the EMRL is calculated using a numerical integration over the probability density function (pdf)  $f_{\gamma}(\gamma)$  over a shift size interval ranging from  $\gamma_{\min}$  (the integral's lower limit) to  $\gamma_{\max}$  (the integral's upper limit). By assuming a continuous uniform distribution over the interval  $(\gamma_{\min}, \gamma_{\max})$  [35], the pdf  $f_{\gamma}(\gamma)$  is defined as  $f_{\gamma}(\gamma) = \frac{1}{(\gamma_{\max} - \gamma_{\min})}$  where  $\gamma_{\max} - \gamma_{\min}$  represents the interval length. The values for the expected average run length (EARL) and the expected average sample size (EASS) can therefore also be calculated using [28]

$$EARL = \int_{\gamma_{\min}}^{\gamma_{\max}} f_{\gamma}(\gamma) ARL(\gamma) d\gamma \quad (15)$$

and

$$EASS = \int_{\gamma_{\min}}^{\gamma_{\max}} f_{\gamma}(\gamma) ASS(\gamma) d\gamma \quad (16)$$

correspondingly.

#### 4. Optimization Designs Procedure

This section presents the computation procedures for determining the optimal charting parameters for the SDS  $np$  chart, under both ZS and SS modes, to minimize the (i)  $MRL_1$  (described in Section 4.1) and (ii)  $EMRL_1$  (described in Section 4.2).

##### 4.1. Computation of the Optimal Charting Parameter for the SDS $np$ Chart to Minimize $MRL_1$

In this section, the optimal charting parameters ( $n_1, n_2, W, L_1, L_2, H$ ) of the SDS  $np$  chart, under both ZS and SS modes, is obtained by minimizing  $MRL_1(\gamma_{opt})$  subject to the achievement of minimum IC MRL ( $MRL_{0min}$ ) and predetermined IC ASS ( $ASS_0$ ), for a rapid detection  $\gamma_{opt}$  is required. Note that  $\gamma_{opt}$  represents the desired size of a fraction nonconforming shift. The optimization model in Tuh et al. [14] is adopted in this study to compute the optimal charting parameter ( $n_1, n_2, W, L_1, L_2, H$ ) combination when IC minimum ( $MRL_{0min}$ ) is 370.4. The following is a mathematical formulation of the optimization model:

$$\min_{n_1, n_2, W, L_1, L_2, H} MRL_1(\gamma_{opt}) \quad (17)$$

subject to

$$MRL_0 \geq MRL_{0min} \quad (18)$$

and

$$ASS_0 = n. \quad (19)$$

In view of the distinct nature of RL random variable, it is crucial to emphasize herein that MRL takes the form of an integer. Consequently, the occurrence of multiple ( $n_1, n_2, W, L_1, L_2, H$ ) combinations with similar minimum  $MRL_1$  at a particular  $\gamma_{opt}$  may be observed. In such a scenario, the optimal ( $n_1, n_2, W, L_1, L_2, H$ ) combination having the lowest  $ASS_1$  is preferred.

The procedure for searching the optimal ( $n_1, n_2, W, L_1, L_2, H$ ) combination, based on the optimization model in (17)–(19) of the SDS  $np$  chart based on MRL, is outlined as follows:

- Step 1: Specify the  $p_0, n, MRL_{0min}$  and  $\gamma_{opt}$  values. Here,  $n$  is the average sample size at every sampling stage when the process is in an IC state.
- Step 2: Set  $H$  to one at the start.
- Step 3: Set the initial value of  $MRL_{1min}$  to  $10^5$  (a relatively large value).
- Step 4: Start with  $n_1$  equal to one.
- Step 5: With the current  $n_1$  value, the combination of ( $n_1, n_2, W, L_1, H$ ) is determined for a specified  $n$  when  $\gamma = 1$ , such that the Constraint (19) is fulfilled. The value of  $n_2$  is obtained by rearranging Equation (13), i.e.,  $n_2 = \frac{(n-n_1)}{P(\lfloor W \rfloor < d_{1,i} < \lfloor L_1 \rfloor)}$ , and is rounded up to the nearest integer, where  $0 < W < L_1$ .
- Step 6: For the ZS mode,  $L_2$  is determined via Constraint (18) together with Equations (5) and (10). For the SS mode, on the other hand,  $L_2$  can be obtained by solving Constraint (18) together with Equations (6) and (10). The computed MRL equals to  $MRL_0$  when  $\gamma = 1$  (i.e.,  $p = p_0$ ), where  $L_2 > L_1$ . In this step, the possible ( $n_1, n_2, W, L_1, L_2, H$ ) combination is identified.
- Step 7: Once the possible ( $n_1, n_2, W, L_1, L_2, H$ ) combination is determined,  $MRL_1$  will be computed for  $p = p_1$ , by means of Equations (5) and (10) (for ZS mode) or Equations (6) and (10) (for SS mode). If the computed  $MRL_1$  is less than the present  $MRL_{1min}$ , substitute the newly computed  $MRL_1$  for the  $MRL_{1min}$  value. The ( $n_1, n_2, W, L_1, L_2, H$ ) combination is saved temporarily as the possible combination. If the ( $n_1, n_2, W, L_1, L_2, H$ ) combination found in the following searching produces identical  $MRL_{1min}$ , it will be kept together as a possible combination. Otherwise, if the ( $n_1, n_2, W, L_1, L_2, H$ ) combination results in a larger  $MRL_1$  value, it will be ignored.
- Step 8: Once the search with  $n_1 = 1$  is complete,  $n_1$  is increased by one. Repeat Steps 5–7 for each remaining  $n_1 = 2, 3, \dots, (n - 1)$ , in order to find the possible ( $n_1, n_2, W, L_1, L_2,$



$H$ ) combinations that fulfil the Constraints (18) and (19) and having the lowest value of  $MRL_1$ .

Step 9: If  $MRL_{1min}$  value has been reduced, increase  $H$  by 1 and repeat Steps 3–8. Else, proceed to Step 10.

Step 10: If more than one combination of  $(n_1, n_2, W, L_1, L_2, H)$  delivers a similar minimum  $MRL_{1min}$  value, the combination that produces the smallest OOC average sample size ( $ASS_1$ ) value is chosen as the optimal combination. Additionally, if more than one combination of  $(n_1, n_2, W, L_1, L_2, H)$  produces similar comparable lowest pair values ( $MRL_1, ASS_1$ ), the parameters combination corresponding to the lowest  $H$  is taken to be the optimal combination in this case.

Two MATLAB programs are written to compute the optimal  $(n_1, n_2, W, L_1, L_2, H)$  combination for the SDS  $np$  chart, each for the ZS and SS mode apiece, based on the set of input parameters ( $MRL_{0min}, \gamma_{opt}, n, p_0$ ).

#### 4.2. Computation of the Optimal Charting Parameter for the SDS $np$ Chart to Minimize $EMRL_1$

The MRL-based design (discussed in Section 4.1) can only be implemented if shift size  $\gamma$  can be specified beforehand. By using the method in this section, the optimal charting parameters that improve the sensitivity of the SDS  $np$  chart can be obtained even though the exact shift size is not known.

The formulation for the optimization model for the SDS  $np$  chart with unknown shift sizes is as follows:

$$\min_{n_1, n_2, W, L_1, L_2, H} EMRL_1 \quad (20)$$

subject to

$$EMRL_0 \geq MRL_{0min} \quad (21)$$

and

$$EASS_0 = n \quad (22)$$

Below is a detailed explanation of the procedure to compute the optimal charting parameters.

Step 1: Specify the desired values of  $\gamma_{min}, \gamma_{max}, n, p_0$ , and  $MRL_{0min}$ .

Step 2: Similar to Steps 2 to 5 of the optimization procedure outlined in Section 5.1, but  $\downarrow$  with

Step 5: Constraints (21) and (22) in place of Constraints (18) and (19) by minimizing the OOC EMRL ( $EMRL_1$ ) in Equation (20).

Step 6: For the ZS mode,  $L_2$  is based on the Equations (5) and (10) and Constraint (21), in which the computed EMRL equals to  $EMRL_0$  (i.e., when  $p = p_0$ ), where  $L_2 > L_1$ .

Note that for the case of SS mode, on the other hand,  $L_2$  can be obtained by solving Constraint (21) together with Equations (6) and (10). The non-integer setting of  $W, L_1$  and  $L_2$  are based on operating procedure of DS sub-chart as described in Section 2. In this step, the possible parameters  $(n_1, n_2, W, L_1, L_2, H)$  combination is identified.

Step 7: Once the possible  $(n_1, n_2, W, L_1, L_2, H)$  combination has been identified,  $EMRL_1$  is calculated (i.e., when  $p = p_1$ ), by means of Equations (5), (10) and (14) (for ZS mode) or Equations (6), (10) and (14) (for SS mode). If the calculated  $EMRL_1$  is lower than the present  $EMRL_{1min}$ , substitute the newly computed  $EMRL_1$  for the  $EMRL_{1min}$  value. The current  $(n_1, n_2, W, L_1, L_2, H)$  combination is temporarily saved as the possible combination. If the combination  $(n_1, n_2, W, L_1, L_2, H)$  obtained in the subsequent searching produces an  $EMRL_{1min}$  that is comparable to the one being searched for, the combination will be saved as a possible one. If this is not the case, the combination  $(n_1, n_2, W, L_1, L_2, H)$  will be disregarded if the  $EMRL_1$  value that it produces is higher.

Step 8: Increase  $n_1$  by one when the search is finished with  $n_1 = 1$ . For the remaining  $n_1 = 2, 3, \dots, (n - 1)$ , repeat Steps 5 through 7, to look for the possible  $(n_1, n_2, W, L_1, L_2, H)$  combinations that fulfil Constraints (21)–(22) and have the lowest value of  $EMRL_1$ .

Step 9: If the  $EMRL_{1min}$  value has been lowered, raise  $H$  by 1 and repeat Steps 3–8. Otherwise, move on to Step 10.

Step 10: If multiple combinations of  $(n_1, n_2, W, L_1, L_2, H)$  give a similar minimum  $EMRL_{1min}$  value, the optimal combination is the one that produces the lowest OOC expected average sample size ( $EASS_1$ ) value. Additionally, if more than one combination of  $(n_1, n_2, W, L_1, L_2, H)$  produces a similar comparable lowest pair ( $EMRL_1, EASS_1$ ) value, the parameter combination corresponding to the lowest  $H$  is taken to be the optimal combination in this case.

Two MATLAB programs are written to compute the optimal  $(n_1, n_2, W, L_1, L_2, H)$  combination for the EMRL-based SDS  $np$  chart, for the ZS and SS modes, individually, based on desired values of  $\gamma_{min}$ ,  $\gamma_{max}$ ,  $n$ ,  $p_0$ , and  $MRL_{0min}$ . The numerical integration method based on the Gauss Legendre Quadrature rule is employed in this section to compute the integral involve computations, for designing EMRL-based SDS  $np$  chart. The values of weights ( $w_i$ ) and nodes ( $x_i$ ) can be obtained using the MATLAB coding written by Winckel [36], which is borrowed to build the MATLAB programs for the computations of  $EMRL_1$  (or  $E(\ell_{0.5})_1$ ),  $EARL_1$ , and  $EASS_1$ . Here, a value of  $N$  equal to 200 is used for the number of ordinates, following Tuh et al. [28].

## 5. Comparative Studies

This section is divided into two subsections. The comparison studies of the SDS  $np$  chart with the optimal synthetic  $np$  and optimal DS  $np$  charts in both ZS and SS modes, based on MRL and EMRL (for known and unknown shift sizes cases), are covered in Sections 5.1 and 5.2, respectively.

### 5.1. Performance Analysis of the SDS $np$ Chart Based on MRL

In this section, the performance of the SDS  $np$  chart is evaluated using MRL as the chart's performance criterion. The IC MRL ( $MRL_0$ ) and the OOC MRL ( $MRL_1$ ) are the two types of MRLs that are frequently used. The  $MRL_1$  value should be low in a good control chart to allow for quick detection of an OOC condition, while the  $MRL_0$  value should be large to prevent overly frequent false alarms. The different input parameter combinations from  $MRL_{0min} = \{370.4\}$ ,  $IC\ p_0 = \{0.005, 0.01, 0.02\}$ ,  $n = \{25, 50, 100, 200, 400, 800\}$  and shift size  $\gamma_{opt} = \{1.5, 2.0, 3.0\}$  are considered. The input combination parameters applied in this work have been adopted by De Araujo Rodrigues et al. [29], Chong et al. [13] and Lee and Khoo [37] for use in their own research on DS  $np$ , SDS  $np$  and synthetic  $np$  charts, respectively. The code developed herein has also been tested with the optimal charting parameters for SDS  $np$  chart based on ARL developed by Chong et al. [13], with exact similar output (ARL and ASS values) obtained, henceforth confirming the validity and reliability of the methodology.

The optimal charting parameters  $(n_1, n_2, W, L_1, L_2, H)$  of the SDS  $np$  chart, in ZS and SS, as well as the corresponding  $MRL_0$  and  $ARL_0$  are presented in Table 1. These optimal charting parameters  $(n_1, n_2, W, L_1, L_2, H)$  aid quality practitioners to choose the optimal parameters of the MRL-based SDS  $np$  chart in the implementation of the SDS  $np$  chart. For example, when the process is in SS mode,  $\gamma_{opt} = 2.0$ ,  $p_0 = 0.01$  and  $n = 50$ , optimal parameters  $(n_1, n_2, W, L_1, L_2, H) = (16, 229, 0.5, 2.5, 5.5, 11)$ . In addition, Table 1 gives a comparison between the  $ARL_0$  and  $MRL_0$  values of the SDS  $np$  chart. It is noted that all the  $MRL_0$  values are smaller than the corresponding  $ARL_0$  values.

Numerical comparison in Table 2 shows that there is a significant difference between the  $MRL_1$  and  $ARL_1$  values of the SDS  $np$  chart, for both ZS and SS modes. For example,  $MRL_1 = 11$  when  $\gamma_{opt} = 1.5$ ,  $p_0 = 0.005$  and  $n = 100$ ,  $MRL_{0min} = 370.4$  and in the ZS mode implies that the SDS  $np$  chart gives an OOC signal not later than the 11th sample about half of the time, although  $ARL_1 = 32.13$ . Interestingly, the SDS  $np$  chart's SS  $MRL_1$  is seen to be larger than the ZS  $MRL_1$ . This suggests that because its head-start feature is no longer present, its SS performance is worse than the ZS performance.

**Table 1.** Optimal charting parameters for the MRL-based SDS  $np$  chart, in ZS and SS modes, together with their corresponding values of  $MRL_0$  and  $ARL_0$ , when  $RL_{0min} = 370.4$ .

$\gamma_{opt}$	$p_0$	$n$	ZS	SS				
			$(n_1, n_2, W, L_1, L_2, H)$	$MRL_0$	$ARL_0$	$(n_1, n_2, W, L_1, L_2, H)$	$MRL_0$	$ARL_0$
1.5	0.005	100	(25, 636, 0.5, 3.5, 6.5, 11)	375	580.45	(18, 951, 0.5, 2.5, 8.5, 26)	378	544.97
		200	(40, 880, 0.5, 3.5, 8.5, 7)	400	608.15	(91, 1427, 1.5, 4.5, 12.5, 29)	383	552.31
		400	(46, 1719, 0.5, 3.5, 13.5, 4)	374	562.28	(152, 1404, 1.5, 5.5, 13.5, 16)	374	539.96
		800	(457, 1744, 3.5, 8.5, 16.5, 2)	376	557.36	(198, 2310, 1.5, 7.5, 19.5, 9)	371	535.20
	0.01	50	(10, 418, 0.5, 2.5, 7.5, 11)	375	580.09	(8, 543, 0.5, 3.5, 9.5, 41)	397	572.40
		100	(20, 439, 0.5, 3.5, 8.5, 7)	413	627.46	(47, 659, 1.5, 4.5, 11.5, 17)	382	551.47
		200	(126, 564, 2.5, 5.5, 11.5, 4)	378	566.98	(76, 703, 1.5, 5.5, 13.5, 16)	377	543.74
		400	(166, 1016, 2.5, 6.5, 17.5, 2)	391	579.12	(99, 1155, 1.5, 6.5, 19.5, 9)	376	542.89
	0.02	25	(5, 208, 0.5, 2.5, 7.5, 11)	396	610.51	(4, 270, 0.5, 2.5, 9.5, 43)	406	584.77
		50	(10, 219, 0.5, 2.5, 8.5, 7)	400	607.77	(24, 315, 1.5, 4.5, 11.5, 25)	392	565.75
		100	(44, 254, 1.5, 6.5, 10.5, 4)	382	573.43	(38, 354, 1.5, 4.5, 13.5, 14)	375	540.14
		200	(115, 431, 3.5, 7.5, 16.5, 2)	399	590.67	(51, 548, 1.5, 6.5, 18.5, 6)	386	556.41
	0.005	100	(39, 345, 0.5, 2.5, 4.5, 4)	414	620.41	(33, 441, 0.5, 2.5, 5.5, 13)	398	574.43
		200	(185, 287, 2.5, 3.5, 5.5, 3)	412	614.77	(122, 626, 1.5, 4.5, 7.5, 9)	379	547.17
		400	(385, 469, 4.5, 5.5, 8.5, 4)	411	616.25	(295, 571, 2.5, 6.5, 8.5, 4)	384	553.92
		800	(362, 869, 1.5, 4.5, 12.5, 1)	373	548.07	(703, 829, 5.5, 7.5, 14.5, 2)	380	548.66
2.0	0.01	50	(19, 179, 0.5, 2.5, 4.5, 4)	371	557.17	(16, 229, 0.5, 2.5, 5.5, 11)	401	578.69
		100	(92, 155, 2.5, 3.5, 5.5, 3)	386	575.39	(61, 314, 1.5, 4.5, 7.5, 9)	380	548.12
		200	(192, 253, 4.5, 5.5, 8.5, 4)	383	575.35	(143, 335, 2.5, 5.5, 9.5, 7)	379	546.40
		400	(182, 429, 1.5, 4.5, 12.5, 1)	376	552.38	(351, 421, 5.5, 7.5, 14.5, 2)	387	557.61
	0.02	25	(6, 175, 0.5, 1.5, 6.5, 4)	393	589.85	(8, 114, 0.5, 2.5, 5.5, 2)	395	569.72
		50	(46, 78, 2.5, 3.5, 5.5, 3)	403	600.33	(29, 188, 1.5, 3.5, 8.5, 11)	411	593.04
		100	(96, 128, 4.5, 5.5, 8.5, 4)	398	597.17	(75, 134, 2.5, 5.5, 8.5, 5)	373	537.64
		200	(92, 210, 1.5, 4.5, 12.5, 1)	378	555.17	(176, 205, 5.5, 7.5, 14.5, 2)	410	591.77
	0.005	100	(91, 137, 1.5, 2.5, 3.5, 4)	397	596.05	(90, 155, 1.5, 2.5, 3.5, 4)	388	559.79
		200	(152, 354, 1.5, 2.5, 7.5, 1)	373	548.49	(153, 275, 1.5, 3.5, 5.5, 5)	393	566.75
		400	(153, 500, 0.5, 2.5, 10.5, 1)	379	557.69	(150, 511, 0.5, 2.5, 8.5, 1)	376	542.55
		800	(254, 802, 0.5, 3.5, 12.5, 1)	395	581.14	(254, 802, 0.5, 3.5, 12.5, 1)	419	604.29
	0.01	50	(32, 66, 0.5, 2.5, 3.5, 7)	389	592.05	(44, 96, 1.5, 2.5, 4.5, 10)	410	591.51
		100	(76, 177, 1.5, 2.5, 7.5, 1)	381	560.19	(76, 141, 1.5, 3.5, 5.5, 5)	385	555.44
		200	(77, 247, 0.5, 2.5, 10.5, 1)	375	551.78	(131, 206, 1.5, 3.5, 9.5, 1)	373	537.46
		400	(125, 405, 0.5, 3.5, 11.5, 1)	377	553.85	(126, 403, 0.5, 3.5, 11.5, 1)	385	555.39
3.0	0.02	25	(22, 48, 1.5, 2.5, 3.5, 3)	377	562.22	(10, 82, 0.5, 3.5, 4.5, 7)	372	536.59
		50	(38, 88, 1.5, 2.5, 7.5, 1)	399	585.89	(38, 70, 1.5, 3.5, 5.5, 5)	416	600.56
		100	(38, 125, 0.5, 2.5, 9.5, 1)	405	594.47	(38, 125, 0.5, 2.5, 8.5, 1)	385	555.19
		200	(94, 202, 1.5, 4.5, 13.5, 1)	384	563.94	(94, 202, 1.5, 4.5, 13.5, 1)	407	586.72

**Table 2.** MRL<sub>1</sub> comparison between SDS *np*, DS *np* and synthetic *np* charts with associated ARL<sub>1</sub> of the SDS *np* chart, in ZS and SS modes, when MRL<sub>0min</sub> = 370.4.

$\gamma_{opt}$	$p_0$	$n$	ZS				SS			
			MRL <sub>1</sub>			ARL <sub>1</sub>	MRL <sub>1</sub>			ARL <sub>1</sub>
			Synthetic <i>np</i>	DS <i>np</i>	SDS <i>np</i>		Synthetic <i>np</i>	DS <i>np</i>	SDS <i>np</i>	
1.5	0.005	100	47	26	11	32.13	72	26	25	36.18
		200	32	14	7	21.00	47	14	15	21.19
		400	13	8	4	12.50	25	8	9	12.97
		800	7	4	2	6.79	13	4	5	7.35
	0.01	50	48	26	11	31.06	74	26	25	35.55
		100	32	15	7	21.18	48	15	15	21.93
		200	14	8	4	11.92	25	8	9	12.91
		400	7	4	2	6.79	13	4	5	7.34
	0.02	25	46	25	11	31.38	73	25	25	35.49
		50	34	15	7	20.96	50	15	15	21.46
		100	14	8	4	12.01	26	8	9	12.91
		200	7	4	2	6.82	13	4	5	7.56
2.0	0.005	100	9	9	4	12.20	24	9	9	13.11
		200	5	5	3	9.61	13	5	5	7.37
		400	3	3	2	4.50	6	3	3	4.66
		800	2	2	1	3.73	3	2	2	3.27
	0.01	50	9	9	4	11.53	24	9	9	13.13
		100	5	5	3	9.14	13	5	5	7.32
		200	3	3	2	4.36	6	3	3	4.39
		400	2	2	1	3.79	3	2	2	3.23
	0.02	25	9	9	4	12.53	24	9	9	12.77
		50	5	5	3	9.13	13	5	5	7.25
		100	3	3	2	4.34	6	3	3	4.58
		200	2	2	1	3.88	3	2	2	3.27
	0.005	100	4	3	2	4.31	7	3	4	6.10
		200	2	2	1	3.75	4	2	2	3.01
		400	1	1	1	3.37	2	1	2	3.01
		800	1	1	1	1.43	2	1	2	2.08
	0.01	50	4	3	2	3.71	7	3	4	5.76
		100	2	2	1	3.73	4	2	2	2.97
		200	1	1	1	3.39	2	1	2	3.02
		400	1	1	1	1.28	2	1	2	1.88
	0.02	25	4	3	2	4.26	7	3	3	4.48
		50	2	2	1	3.71	4	2	2	2.95
		100	1	1	1	2.70	2	1	2	3.02
		200	1	1	1	1.27	2	1	2	1.87

The  $MRL_1$  performances of the SDS  $np$  chart are compared with the synthetic  $np$  and DS  $np$  charts in this section. Note that the  $MRL_1$  for the synthetic  $np$  and DS  $np$  charts in Table 2 are taken from Lee and Khoo [37] and Tuh et al. [30], correspondingly. It is clearly seen in Table 2, the SDS  $np$  chart outperforms the synthetic  $np$  and DS  $np$  charts for all shift sizes, in ZS mode, with the SDS  $np$  chart giving lower  $MRL_1$  than the competing charts for identical  $(\gamma_{opt}, p_0, n, MRL_{0min})$  combination. However, when the process is under SS mode, the optimal SDS  $np$  chart surpasses the synthetic  $np$  chart but does not demonstrate considerable improvement in comparison to the DS  $np$  chart in signalling the process fraction nonconforming shift. Overall, the SDS  $np$  chart outperforms the DS  $np$  chart when  $\gamma_{opt} = 1.5$  and  $np_0 = 0.5$  for different combinations of  $(n, p_0) = (100, 0.005)$  and  $(50, 0.01)$ . This result is consistent with the conclusion reached by Costa and Machado [5]. They used SS ARL to measure the performance of the SDS  $\bar{X}$  chart.

### 5.2. Performance Analysis of the SDS $np$ Chart Based on EMRL

The SDS  $np$  chart's optimal charting parameters  $(n_1, n_2, W, L_1, L_2, H)$ , can be achieved by minimizing the OOC expected median run length ( $EMRL_1$ ), are shown in Tables 3 and 4. In Table 5, the  $EMRL_1$  performance of the synthetic  $np$ , DS  $np$  and SDS  $np$  charts are compared. The process in ZS and SS modes are considered. The parameter combinations of  $MRL_{0min} = 370.4$ ,  $p_0 \in \{0.005, 0.01, 0.02\}$ ,  $n \in \{25, 50, 100, 200, 400, 800\}$  and two intervals of process shift sizes: (i)  $(\gamma_{min}, \gamma_{max}] = (1.1, 2.0]$  and (ii)  $(\gamma_{min}, \gamma_{max}] = (2.0, 3.0]$ . Results presented in the columns 8–10 of Tables 3 and 4 were extracted from the work by Tuh et al. [28] in order to provide clear performance comparison discussions herein. They used EMRL to measure the performance of DS  $np$  chart. Two MATLAB programs that incorporate the optimization procedure described in Lee and Khoo [37], by means of minimizing  $EMRL_1$  is written to compute the optimal charting parameters for the synthetic  $np$  chart, based on the ZS and SS modes, individually. The optimal charting parameters and corresponding  $EMRL_0$  and  $EARL_0$  values are displayed in columns 5–7 of Tables 3 and 4.

For example, Table 3 demonstrates that when the process is in ZS mode with  $p_0 = 0.01$ ,  $MRL_{0min} = 370.4$ ,  $n = 100$  and  $(\gamma_{min}, \gamma_{max}] = (1.1, 2.0]$ , optimal synthetic  $np$ , optimal DS  $np$  and optimal SDS  $np$  charts give  $(UCL_S, H_S) = (3.5, 5)$ ,  $(n_1, n_2, W, L_1, L_2) = (27, 2454, 1.5, 4.5, 34.5)$  and  $(n_1, n_2, W, L_1, L_2, H) = (34, 1453, 1.5, 4.5, 20.5, 37)$ , correspondingly. The lowest  $EMRL_1$  (listed in Table 5) value is produced by the synthetic  $np$ , DS  $np$  and SDS  $np$  charts with these optimal charting parameters, while the  $EMRL_0$  is at least 370.4. Subsequently, the corresponding values of  $(EMRL_0, EARL_0)$  for the optimal synthetic  $np$ , DS  $np$  and SDS  $np$  chart, are computed as (408, 614.58), (385, 554.77) and (371, 613.95), individually.

In Table 5, the  $EMRL_1$  and  $EARL_1$  values for the OOC case, in ZS and SS modes, can be obtained using the optimal charting parameters of the synthetic  $np$ , DS  $np$  and SDS  $np$  charts (in Tables 3 and 4). For instance, when  $p_0 = 0.005$ ,  $n = 200$ ,  $MRL_{0min} = 370.4$  and  $(\gamma_{min}, \gamma_{max}] = (2.0, 3.0]$ , Table 4 gives  $(n_1, n_2, W, L_1, L_2, H) = (130, 506, 1.5, 5.5, 6.5, 5)$  as the optimal charting parameters for the SDS  $np$  chart. With these optimal charting parameters,  $(EMRL_1, EARL_1) = (3.47, 4.54)$  when process is in SS mode. Numerical results in Tables 3 and 4 clearly show that the  $EMRL_0$  values are lower than  $EARL_0$  of the optimal SDS  $np$  chart when the process is IC ( $\gamma = 1$ ). For instance, when the process is in ZS mode, the SDS  $np$  chart gives  $EARL_0 = 610.92$  when  $p_0 = 0.01$ ,  $n = 200$ ,  $(\gamma_{min}, \gamma_{max}] = (1.1, 2.0]$  and  $MRL_{0min} = 370.4$  (in Table 3). Practitioners might conclude that a false alarm occurs to every 610,92th sample fifty percent of the time. In reality, this value lies between the 60th (=535) and 70th (=746) percentiles of the RL distribution, and the false alarm occurs prior to the 610.92nd sample, or by the 372nd sample ( $EMRL_0 = 372$ ), fifty percent of the time.

On the other hand, for the OOC condition (see Table 5), in ZS mode, when  $p_0 = 0.02$ ,  $n = 100$ ,  $(\gamma_{min}, \gamma_{max}] = (2.0, 3.0]$  and  $MRL_{0min} = 370.4$ , the SDS  $np$  chart gives  $EARL_1 = 16.92$ , while  $EMRL_1 = 9.13$ , showing a trivial difference between the  $EARL_1$  and  $EMRL_1$  values. This indicates that when there is a substantial amount of right-skewed in the RL distribution, the average is significantly higher than the median. On the other hand, when there is symmetric distribution, the average is located quite near to the median.



As a result of this, the use of EMRL is advised as a performance metric rather than the EARL because the EMRL provides a more understandable interpretation for the performance SDS  $np$  chart.

Results in Table 5 demonstrate that the SS EMRL<sub>1</sub> is larger than ZS EMRL<sub>1</sub> in all interval shift sizes of the SDS  $np$  chart. This indicates that the SS EMRL<sub>1</sub> performance of the SDS  $np$  chart is worse than its ZS performance. This is due to the fact that the SS performance calculates how long it will take for the SDS  $np$  chart to signal in this case once the head-start's effects have gradually disappeared. As can be seen in Table 5, the optimal SDS  $np$  chart outperforms the synthetic  $np$  and DS  $np$  charts for all shift sizes  $(\gamma_{\min}, \gamma_{\max}]$ , under ZS mode, with the SDS  $np$  chart giving lower EMRL<sub>1</sub> than the competing charts for identical  $p_0$ ,  $n$ , MRL<sub>0min</sub> and  $(\gamma_{\min}, \gamma_{\max}]$  combination. When the process is in SS mode, the SDS  $np$  chart surpasses the synthetic  $np$  chart while performing differently compared to the DS  $np$  chart. Table 5 also demonstrates that the SDS  $np$  chart does not perform any better than the DS  $np$  chart in identifying process fraction nonconforming shifts, particularly those with large shift sizes interval  $(\gamma_{\min}, \gamma_{\max}] = (2.0, 3.0]$ . This observation is in good agreement with the results reported by Costa and Machado [5], where they studied the SS behaviour of the synthetic and side-sensitive synthetic double sampling charts.

**Table 3.** Optimal charting parameters for the SDS  $np$ , synthetic  $np$  and DS  $np$  charts, based on EMRL, in ZS mode, together with their corresponding MRL<sub>0</sub> and EARL<sub>0</sub> values, when MRL<sub>0min</sub> = 370.4.

$\gamma_{\min}$	$\gamma_{\max}$	$p_0$	$n$	Synthetic $np$		DS $np$		SDS $np$					
				(UCL $_S$ , H $_S$ )	EMRL $_0$	EARL $_0$	$(n_1, n_2, W, L_1, L_2)$	EMRL $_0$	EARL $_0$	$(n_1, n_2, W, L_1, L_2, H)$	EMRL $_0$	EARL $_0$	
1.1	2.0	0.005	100	(2.5, 9)	385	590.91	(38, 3985, 1.5, 3.5, 27.5)	393	566.84	(13, 1379, 0.5, 2.5, 11.5, 53)	372	633.82	
			200	(3.5, 5)	395	594.89	(59, 3979, 1.5, 4.5, 29.5)	375	540.25	(73, 2441, 1.5, 5.5, 18.5, 47)	374	630.58	
			400	(5.5, 7)	371	565.02	(144, 7069, 2.5, 7.5, 48.5)	372	536.36	(178, 3653, 2.5, 7.5, 26.5, 32)	372	608.27	
			800	(8.5, 4)	387	581.47	(374, 10324, 4.5, 10.5, 69.5)	372	536.07	(324, 5869, 3.5, 9.5, 40.5, 23)	376	601.11	
	0.01	50	(2.5, 9)	401	614.90	(23, 1230, 1.5, 3.5, 19.5)	393	566.43	(4, 1167, 0.5, 3.5, 16.5, 67)	371	646.62		
		100	(3.5, 5)	408	614.58	(27, 2454, 1.5, 4.5, 34.5)	385	554.77	(34, 1453, 1.5, 4.5, 20.5, 37)	371	613.95		
		200	(5.5, 7)	384	583.76	(66, 4670, 2.5, 6.5, 60.5)	382	551.07	(49, 1747, 1.5, 5.5, 25.5, 34)	372	610.92		
		400	(8.5, 4)	399	597.97	(189, 4974, 4.5, 10.5, 67.5)	375	541.40	(158, 3221, 3.5, 10.5, 43.5, 25)	372	599.10		
	0.02	25	(2.5, 10)	393	604.97	(11, 719, 1.5, 3.5, 21.5)	371	535.00	(2, 580, 0.5, 2.5, 16.5, 72)	375	657.63		
		50	(3.5, 5)	437	657.15	(13, 1373, 1.5, 4.5, 37.5)	383	551.81	(19, 567, 1.5, 5.5, 17.5, 45)	371	623.17		
		100	(5.5, 7)	411	624.13	(37, 1679, 2.5, 8.5, 46.5)	371	534.37	(24, 921, 1.5, 4.5, 26.5, 35)	371	610.23		
		200	(8.5, 4)	423	633.12	(93, 2728, 4.5, 9.5, 72.5)	373	537.32	(84, 1314, 3.5, 9.5, 37.5, 26)	376	605.55		
2.0	3.0	0.005	100	(2.5, 9)	385	590.91	(58, 1223, 1.5, 4.5, 12.5)	389	560.71	(38, 357, 0.5, 3.5, 4.5, 4)	386	579.25	
			200	(3.5, 5)	395	594.89	(98, 1175, 1.5, 5.5, 13.5)	378	544.67	(139, 398, 1.5, 4.5, 5.5, 2)	397	588.41	
			400	(5.5, 6)	433	653.89	(143, 1599, 1.5, 5.5, 17.5)	381	549.64	(184, 920, 1.5, 6.5, 9.5, 2)	373	552.82	
			800	(8.5, 4)	387	581.47	(497, 2850, 4.5, 11.5, 28.5)	372	537.15	(362, 869, 1.5, 4.5, 12.5, 1)	373	548.07	
	0.01	50	(2.5, 9)	401	614.90	(32, 442, 1.5, 4.5, 10.5)	416	599.25	(19, 179, 0.5, 2.5, 4.5, 4)	371	557.17		
		100	(3.5, 5)	408	614.58	(49, 590, 1.5, 5.5, 13.5)	376	542.01	(34, 228, 0.5, 3.5, 5.5, 2)	388	575.09		
		200	(5.5, 7)	384	583.76	(116, 756, 2.5, 7.5, 17.5)	399	575.89	(102, 360, 1.5, 6.5, 8.5, 2)	378	561.09		
		400	(8.5, 4)	399	597.97	(252, 1340, 4.5, 10.5, 27.5)	372	536.00	(182, 429, 1.5, 4.5, 12.5, 1)	376	552.38		
	0.02	25	(2.5, 9)	437	667.82	(16, 225, 1.5, 4.5, 10.5)	399	575.27	(8, 114, 0.5, 2.5, 5.5, 10)	385	592.78		
		50	(3.5, 5)	437	657.15	(26, 253, 1.5, 4.5, 12.5)	387	558.17	(17, 112, 0.5, 3.5, 5.5, 2)	419	620.78		
		100	(5.5, 7)	411	624.13	(58, 381, 2.5, 7.5, 17.5)	395	569.92	(51, 180, 1.5, 5.5, 8.5, 2)	387	574.02		
		200	(8.5, 4)	423	633.12	(126, 675, 4.5, 12.5, 27.5)	371	535.05	(92, 210, 1.5, 4.5, 12.5, 1)	378	555.17		

**Table 4.** Optimal charting parameters for the SDS  $np$ , synthetic  $np$  and DS  $np$  charts, based on EMRL, in SS mode, together with their corresponding MRL<sub>0</sub> and EARL<sub>0</sub> values, when MRL<sub>0min</sub> = 370.4.

$\gamma_{\min}$	$\gamma_{\max}$	$p_0$	$n$	synthetic $np$		DS $np$		SDS $np$			
				(UCL, H)	EMRL <sub>0</sub>	EARL <sub>0</sub>	( $n_1, n_2, W, L_1, L_2$ )	EMRL <sub>0</sub>	EARL <sub>0</sub>	( $n_1, n_2, W, L_1, L_2, H$ )	EMRL <sub>0</sub> EARL <sub>0</sub>
1.1	2.0	0.005	100	(2.5, 11)	386	556.01	(38, 3985, 1.5, 3.5, 27.5)	393	566.84	(10, 1840, 0.5, 3.5, 13.5, 63)	373 536.97
			200	(3.5, 6)	382	550.78	(59, 3979, 1.5, 4.5, 29.5)	375	540.25	(77, 2151, 1.5, 5.5, 16.5, 45)	372 535.99
			400	(5.5, 8)	385	555.83	(144, 7069, 2.5, 7.5, 48.5)	372	536.36	(94, 3784, 1.5, 5.5, 26.5, 33)	373 538.41
			800	(8.5, 4)	435	626.65	(374, 10324, 4.5, 10.5, 69.5)	372	536.07	(333, 5334, 3.5, 10.5, 37.5, 27)	371 534.75
		0.01	50	(2.5, 12)	373	537.54	(23, 1230, 1.5, 3.5, 19.5)	393	566.43	(7, 633, 0.5, 2.5, 10.5, 51)	371 534.36
			100	(3.5, 6)	394	568.15	(27, 2454, 1.5, 4.5, 34.5)	385	554.77	(36, 1271, 1.5, 4.5, 18.5, 48)	373 537.57
			200	(5.5, 8)	398	573.32	(66, 4670, 2.5, 6.5, 60.5)	382	551.07	(51, 1610, 1.5, 6.5, 23.5, 30)	371 535.09
			400	(8.5, 4)	446	643.83	(189, 4974, 4.5, 10.5, 67.5)	375	541.40	(165, 2768, 3.5, 9.5, 38.5, 27)	371 535.37
		0.02	25	(2.5, 13)	377	544.15	(11, 719, 1.5, 3.5, 21.5)	371	535.00	(3, 374, 0.5, 2.5, 11.5, 43)	374 539.15
			50	(3.5, 6)	420	605.65	(13, 1373, 1.5, 4.5, 37.5)	383	551.81	(18, 646, 1.5, 4.5, 18.5, 41)	371 535.20
			100	(5.5, 9)	384	553.16	(37, 1679, 2.5, 8.5, 46.5)	371	534.37	(25, 846, 1.5, 5.5, 24.5, 36)	373 537.26
			200	(8.5, 5)	387	558.47	(93, 2728, 4.5, 9.5, 72.5)	373	537.32	(82, 1431, 3.5, 9.5, 39.5, 29)	371 534.99
2.0	3.0	0.005	100	(2.5, 11)	386	556.01	(58, 1223, 1.5, 4.5, 12.5)	389	560.71	(32, 458, 0.5, 3.5, 5.5, 12)	384 553.69
			200	(3.5, 6)	382	550.78	(98, 1175, 1.5, 5.5, 13.5)	378	544.67	(130, 506, 1.5, 5.5, 6.5, 5)	378 545.23
			400	(5.5, 8)	385	555.83	(143, 1599, 1.5, 5.5, 17.5)	381	549.64	(192, 833, 1.5, 6.5, 9.5, 4)	382 550.83
			800	(8.5, 4)	435	626.65	(497, 2850, 4.5, 11.5, 28.5)	372	537.15	(559, 851, 3.5, 6.5, 13.5, 2)	387 558.73
		0.01	50	(2.5, 12)	373	537.54	(32, 442, 1.5, 4.5, 10.5)	416	599.25	(16, 228, 0.5, 3.5, 5.5, 13)	373 538.29
			100	(3.5, 6)	394	568.15	(49, 590, 1.5, 5.5, 13.5)	376	542.01	(65, 254, 1.5, 4.5, 6.5, 5)	373 537.67
			200	(5.5, 8)	398	573.32	(116, 756, 2.5, 7.5, 17.5)	399	575.89	(96, 417, 1.5, 5.5, 9.5, 4)	380 548.67
			400	(8.5, 4)	446	643.83	(252, 1340, 4.5, 10.5, 27.5)	372	536.00	(279, 428, 3.5, 6.5, 13.5, 2)	398 573.67
		0.02	25	(2.5, 13)	377	544.15	(16, 225, 1.5, 4.5, 10.5)	399	575.27	(8, 113, 0.5, 3.5, 5.5, 14)	379 546.74
			50	(3.5, 6)	420	605.65	(26, 253, 1.5, 4.5, 12.5)	387	558.17	(30, 166, 1.5, 4.5, 7.5, 7)	377 543.71
			100	(5.5, 9)	384	553.16	(58, 381, 2.5, 7.5, 17.5)	395	569.92	(48, 208, 1.5, 5.5, 9.5, 4)	402 579.42
			200	(8.5, 5)	387	558.47	(126, 675, 4.5, 12.5, 27.5)	371	535.05	(111, 248, 2.5, 5.5, 12.5, 1)	383 551.69

**Table 5.** EMRL<sub>1</sub> and EARL<sub>1</sub> comparisons between the SDS  $np$ , synthetic  $np$  and DS  $np$  charts, in both ZS and SS modes, when MRL<sub>0min</sub> = 370.4.

$\gamma_{\min}$	$\gamma_{\max}$	$p_0$	$n$	ZS				SS			
				EMRL <sub>1</sub>		EARL <sub>1</sub>		EMRL <sub>1</sub>		EARL <sub>1</sub>	
				Synthetic $np$	DS $np$	SDS $np$		Synthetic $np$	DS $np$	SDS $np$	
1.1	2.0	0.005	100	62.33	38.73	22.17	43.26	77.16	38.73	37.33	52.15
			200	47.98	24.92	14.50	27.45	56.47	24.92	24.83	34.57
			400	27.58	15.88	9.20	17.16	37.76	15.88	16.17	22.34
			800	18.72	9.85	5.59	10.13	26.67	9.85	9.97	13.59
		0.01	50	64.59	39.35	22.61	42.92	74.87	39.35	36.83	51.74
			100	49.35	24.84	14.41	27.44	57.78	24.84	24.83	34.45
			200	28.28	16.13	9.19	17.11	38.52	16.13	16.13	22.28
			400	19.10	9.86	5.58	10.02	27.08	9.86	9.92	13.54

Table 5. Cont.

$\gamma_{\min}$	$\gamma_{\max}$	$p_0$	$n$	ZS			SS				
				EMRL <sub>1</sub>			EARL <sub>1</sub>	EMRL <sub>1</sub>			EARL <sub>1</sub>
				Synthetic $np$	DS $np$	SDS $np$		Synthetic $np$	DS $np$	SDS $np$	
1.1	2.0	0.005	100	62.33	38.73	22.17	43.26	77.16	38.73	37.33	52.15
			200	47.98	24.92	14.50	27.45	56.47	24.92	24.83	34.57
			400	27.58	15.88	9.20	17.16	37.76	15.88	16.17	22.34
			800	18.72	9.85	5.59	10.13	26.67	9.85	9.97	13.59
		0.01	50	64.59	39.35	22.61	42.92	74.87	39.35	36.83	51.74
			100	49.35	24.84	14.41	27.44	57.78	24.84	24.83	34.45
			200	28.28	16.13	9.19	17.11	38.52	16.13	16.13	22.28
			400	19.10	9.86	5.58	10.02	27.08	9.86	9.92	13.54

The numerical and graphical analysis shown in Table 6 and Figure 3, using the optimal parameters by minimizing EMRL<sub>1</sub> to compute the MRL<sub>1</sub> when unknown shift size is an option, providing  $\gamma \in (\gamma_{\min}, \gamma_{\max}]$ , yields remarkable results. The optimal charting parameters for the EMRL-based SDS  $np$  chart can be obtained from Tables 3 and 4.

**Table 6.** MRL<sub>1</sub> values computed using the optimal charting parameters of the EMRL-based SDS  $np$  chart and the MRL-based SDS  $np$  chart for  $n = 100$  and MRL<sub>0min</sub> = 370.4.

$p_0$	Type of SDS $np$ Chart	$(\gamma_{\min}, \gamma_{\max}]$	ZS				SS			
			MRL <sub>1</sub>				MRL <sub>1</sub>			
			$\gamma = 1.2$	$\gamma = 1.5$	$\gamma = 2.0$	$\gamma = 3.0$	$\gamma = 1.2$	$\gamma = 1.5$	$\gamma = 2.0$	$\gamma = 3.0$
0.005	EMRL-based design chart	(1.1, 2.0]	43	16	7	-	81	26	13	-
		(2.0, 3.0]		-	-	2		-	-	4
	MRL-based design chart	-	37	11	4	2	81	25	9	4
0.01	EMRL-based design chart	(1.1, 2.0]	28	10	5	-	56	16	7	-
		(2.0, 3.0]		-	-	1		-	-	2
	MRL-based design chart	-	25	7	3	1	54	15	5	2
0.02	EMRL-based design chart	(1.1, 2.0]	20	6	3	-	37	9	5	-
		(2.0, 3.0]		-	-	1		-	-	2
	MRL-based design chart	-	16	4	2	1	35	9	3	2

The MRL<sub>1</sub> of the MRL-based design chart is presented in Table 6 for the ease of comparison and reference. The computed MRL<sub>1</sub> values can be found in Table 2. The MRL<sub>1</sub> values for both MRL-based and EMRL-based design charts when  $\gamma = 1.2$  are also added to this section for a thorough comparison. Here,  $n = 100$  is chosen for wide coverage to guarantee that all situations are taken into account. As can be observed in Table 6 for the SDS  $np$  chart with EMRL-based design, the MRL<sub>1</sub> computed using  $(n_1, n_2, W, L_1, L_2, H)$  is very close to the MRL<sub>1</sub> computed using specific shift sizes (MRL-based design chart) provided that  $\gamma = (\gamma_{\min}, \gamma_{\max}]$ . For instance, by investigating Tables 3 and 4, when  $n = 100, p_0 = 0.01$  and  $(\gamma_{\min}, \gamma_{\max}] = (1.1, 2.0]$ , the optimal charting parameters for the SDS  $np$  chart is  $(n_1, n_2, W, L_1, L_2, H) = (34, 1453, 1.5, 4.5, 20.5, 37)$  (for ZS mode) or  $(36, 1271, 1.5, 4.5, 18.5, 48)$  (for SS mode), obtained by minimizing EMRL<sub>1</sub>. These optimal charting parameters yield MRL<sub>1</sub> = {28, 10, 5} in ZS mode (or MRL<sub>1</sub> = {56, 16, 7} in SS mode) for  $\gamma = \{1.2, 1.5, 2.0\}$ , while the MRL-based design chart gives MRL<sub>1</sub> = {25, 7, 3} in ZS mode (or MRL<sub>1</sub> = {54, 15, 5} in SS mode).

For better comparison of the MRL- and EMRL-based SDS  $np$  designs under both ZS and SS modes, graphical summaries have also been plotted and furnished in Figure 3. The three SDS  $np$  charts are designed by considering a minimum OOC MRL at  $\gamma \in \{1.2, 1.5, 2.0\}$  shifts. Evidently, when the shift size is close to the value for which they have been designed, the MRL-based SDS  $np$  chart can perform slightly better than the EMRL-based DS  $np$  chart. On the contrary, the EMRL-based DS  $np$  chart performs better than its MRL-based counterpart for all other shift sizes, particularly when the actual shift differs significantly from the specified size. These observations are consistent with the conclusion drawn by Tang et al. [38]. In their work, the performance of EWMA and AEWMA methods at detecting a wide range of shifts are compared. Thus, in the event when  $\gamma \in (\gamma_{\min}, \gamma_{\max}]$ , the optimal parameters provided in Tables 3 and 4 (which are found by minimizing  $EMRL_1$ ) can be used as a substitute for the optimal parameters by assuming a known shift size directly and reliably.

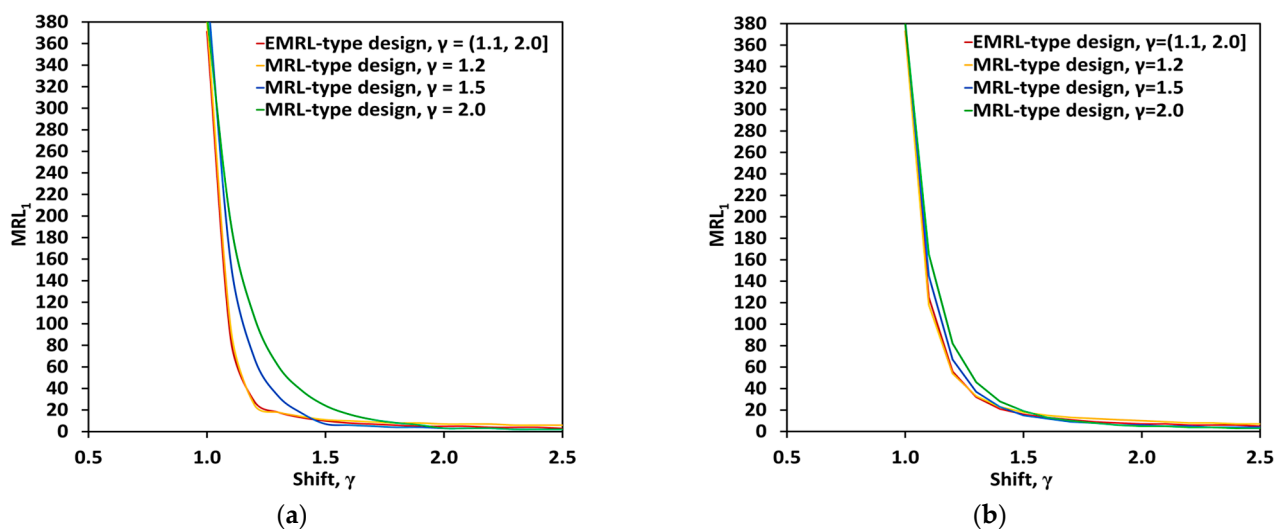


**Figure 3.** Comparison of the MRL values under (a) ZS and (b) SS for MRL- and EMRL-based SDS  $np$  designs.

## 6. An Illustrative Example

In this section, an example is considered to illustrate the implementation of the optimal EMRL-based SDS  $np$  chart. This example can be obtained from Oakland [39]. The data is related to the process of producing ballpoint pen cartridges. The inspected number of defectives found in 50 sample ( $m = 50$ ) of size  $n = 100$  is selected at random every hour from the process is listed in Table 7. Therefore, based on the data, the process fraction nonconforming is computed as 0.02 using the relevant equation,  $\bar{p} = \frac{\sum d}{n}$ .

As illustrated in Figure 4, the  $np$  chart with three-sigma control limits is built in phase I to determine if the process is under control. The centre line (CL), lower control limit (LCL), and upper control limit (UCL) were calculated as follows:

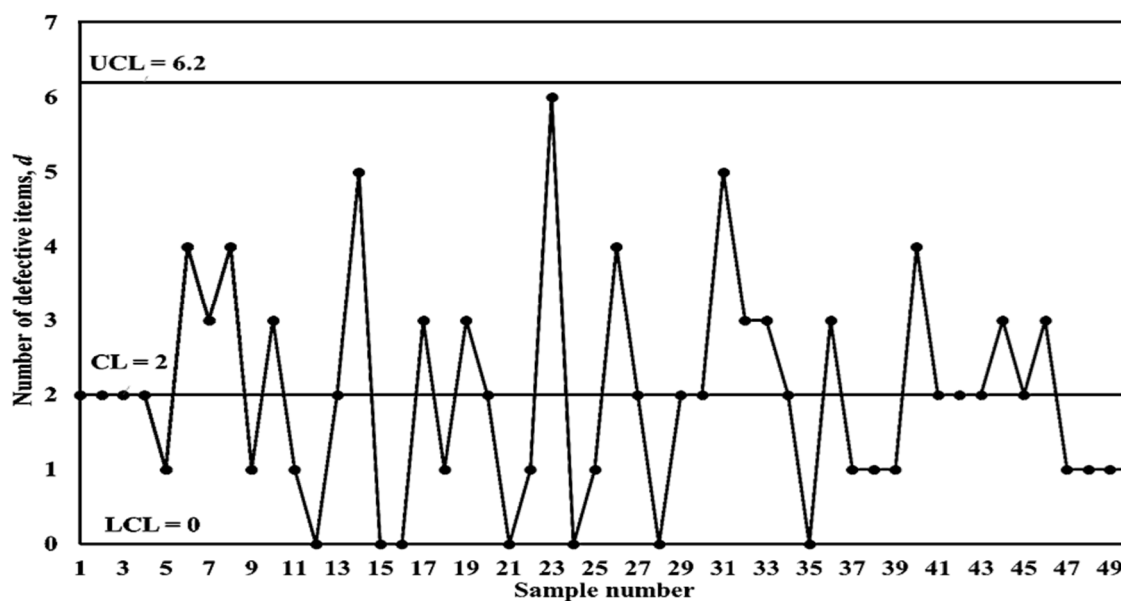
$$CL = n\bar{p} = 100 \times 0.02 = 2$$

$$\begin{aligned} LCL &= n\bar{p} - 3\sqrt{n\bar{p}(1-\bar{p})} \\ &= 100 \times 0.02 - 3\sqrt{100 \times 0.02(1-0.02)} \\ &= -2.2 \\ &\simeq 0 \end{aligned}$$

$$\begin{aligned} UCL &= n\bar{p} + 3\sqrt{n\bar{p}(1-\bar{p})} \\ &= 100 \times 0.02 + 3\sqrt{100 \times 0.02(1-0.02)} \\ &= 6.2 \end{aligned}$$

**Table 7.** Data related to the process of producing ballpoint pen cartridges. Source Oakland [39].

Sample, $j$	Sample Size, $n$	Number of Defectives, $d$	Sample	Sample Size, $n$	Number of Defectives, $d$
1	100	2	26	100	4
2	100	2	27	100	2
3	100	2	28	100	0
4	100	2	29	100	2
5	100	1	30	100	2
6	100	4	31	100	5
7	100	3	32	100	3
8	100	4	33	100	3
9	100	1	34	100	2
10	100	3	35	100	0
11	100	1	36	100	3
12	100	0	37	100	1
13	100	2	38	100	1
14	100	5	39	100	1
15	100	0	40	100	4
16	100	0	41	100	2
17	100	3	42	100	2
18	100	1	43	100	2
19	100	3	44	100	3
20	100	2	45	100	2
21	100	0	46	100	3
22	100	1	47	100	1
23	100	6	48	100	1
24	100	0	49	100	1
25	100	1	50	100	1
			Total	5000	$\sum d = 100$

**Figure 4.** The standard  $np$  with three-sigma control limits.



All the points fall within the control limits, indicating that the process is under control. As a result, the IC process fraction nonconforming ( $p_0$ ) for phase II process monitoring

stage through  $p_0 = \frac{\sum_{j=1}^m p_j}{m} = \frac{\sum_{j=1}^m d_j}{m \times n} = \frac{100}{50 \times 100} = 0.02$  may be estimated.

It is imperative that a significant assignable cause that raises the fraction of nonconforming to 0.028 must be identified as soon as possible. Consequently,  $\gamma = \frac{0.028}{0.02} = 1.4$ . Herein,  $n = 100$ ,  $p_0 = 0.02$ ,  $(\gamma_{\min}, \gamma_{\max}) = (1.1, 2.0]$ , and  $MRL_{0\min} = 370.4$  are preferred. The procedures in Section 2 are adopted to construct the SDS  $np$  chart. The optimal charting parameters of the SDS  $np$  chart by considering the process under SS mode, shown in Table 4 is  $(n_1, n_2, W, L_1, L_2, H) = (25, 846, 1.5, 5.5, 24.5, 36)$ .

The data in Table 8 are simulated using RStudio software; the first ten samples are generated under the IC situation with  $p_0 = 0.02$ , and the next twenty samples are generated under the OOC situation with  $p_1 = 0.028$ . At the first stage of the DS sub-chart, a binomial distribution with parameters  $(n_1, p_0) = (25, 0.02)$  for the IC situation and  $(n_1, p_1) = (25, 0.028)$  for the OOC situation is used to simulate the number of nonconforming items  $d_1$  depicted on the DS  $np$  sub-chart. The number of nonconforming items  $d_2$  depicted at the second stage of the DS  $np$  sub-chart is determined by the parameters of the binomial distribution, which are  $(n_2, p_0) = (846, 0.02)$  for the IC and  $(n_2, p_1) = (846, 0.028)$  for the OOC situations, respectively.

**Table 8.** Simulated dataset for the EMRL-based SDS  $np$  chart.

Sampling Stage, $i$	First Sample ( $n_1 = 25$ ) $d_1$	Second Sample ( $n_2 = 846$ ) $d_2$	$d_1 + d_2$	CRL
1	1			
2	0			
3	0			
4	1			
5	0			
6	0			
7	0			
8	0			
9	1			
10	0			
11	2	29	31	1
12	0			
13	0			
14	1			
15	0			
16	1			
17	0			
18	0			
19	1			
20	0			
21	1			
22	0			

Table 8. Cont.

Sampling Stage, $i$	First Sample ( $n_1 = 25$ ) $d_1$	Second Sample ( $n_2 = 846$ ) $d_2$	$d_1 + d_2$	CRL
23	1			
24	1			
25	1			
26	3	35	38	15
27	0			
28	2	31	33	2
29	2	32	34	1
30	0			

The thirty sampling stages in Table 8 are plotted on the DS  $np$  sub-chart in Figure 5a. One can see that the process stays at the stage 1 of the DS sub-chart for sampling stages 1 through 10, as the points lie below 1.5 ( $<W$ ) are considered to be conforming. At the sampling stage  $i=11$ , a first sample of size  $n_1 = 25$  is taken and  $d_1 = 2$  nonconforming items are observed. As  $d_1 = 2$  falls in the interval  $W < d_1 < L_1$ , take the second sample of size  $n_2 = 846$  and number of nonconforming  $d_2 = 29$  is observed and yields  $d_1 + d_2 = 31$  (see Table 8). Sampling stage  $i = 11$  is categorised as nonconforming because  $d_1 + d_2 > L_2$  ( $L_2 = 24.5$ ). To investigate the process condition further (whether the condition is IC or OOC), the CRL sub-chart (Figure 5b) is required. The number of conforming sampling stages between two non-conforming ones (including the present nonconforming stage) is computed as  $CRL = 1$ . The first OOC signal appears at sampling stage 11 because  $CRL = 1 < H = 36$ .

The process of taking the first sample and likely the second, for each sampling stages is continued until sampling stage  $i = 26$ , here  $d_1 + d_2 = 38$  is seen for  $d_1 = 3$  ( $W < d_1 < L_1$ ) and  $d_2 = 35$ . Hence, sampling stage  $i = 26$  is categorised as nonconforming because  $d_1 + d_2 > L_2$ . The nonconforming sampling stages are also seen at sampling stages  $i = 28$  and 29. This leaves the nonconforming sampling stages of  $i = 11, 26, 28$ , and 29 as OOC states.

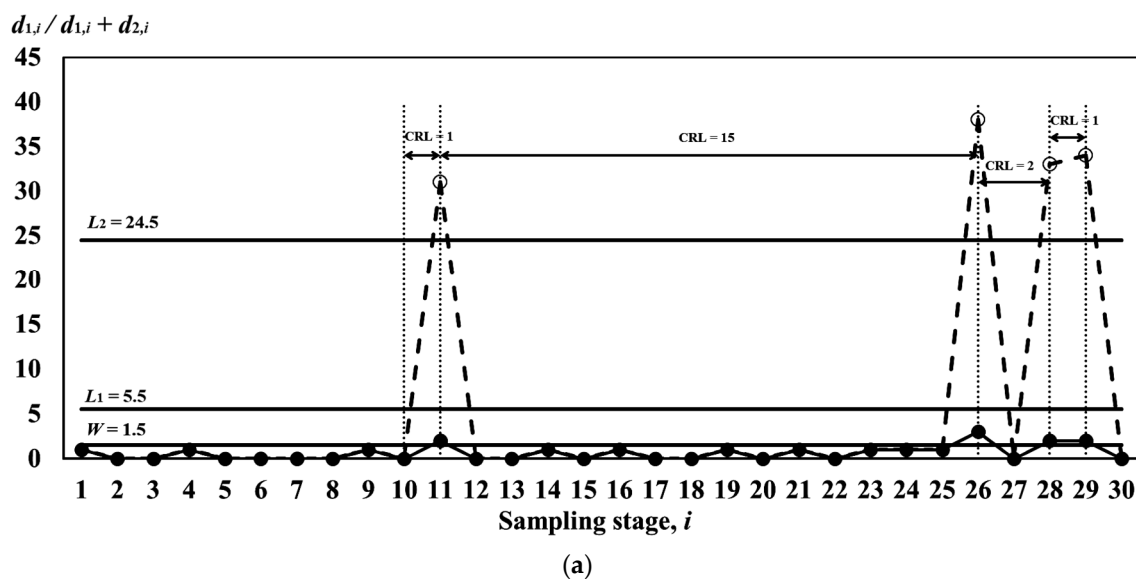
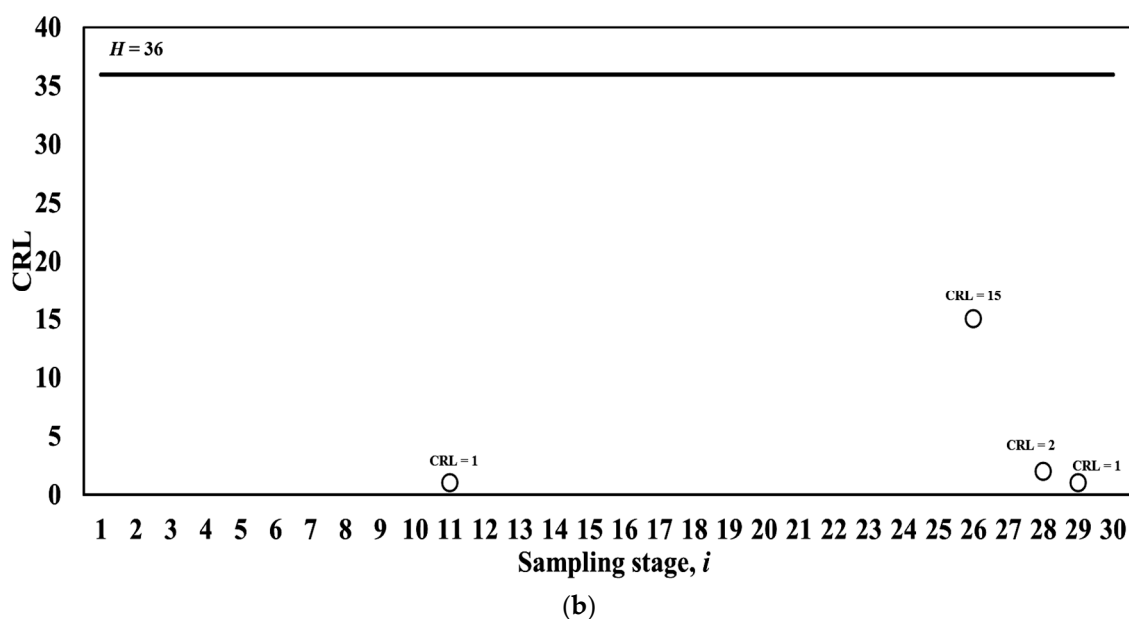


Figure 5. Cont.



**Figure 5.** (a) DS  $np$  sub-chart of the SDS  $np$  chart for minimizing EMRL<sub>1</sub>. (b) CRL sub-chart of the SDS  $np$  chart for minimizing EMRL<sub>1</sub>.

## 7. Conclusions

This study investigates the MRL and EMRL performances of the SDS control chart for detecting increasing shifts in process fraction nonconforming. When compared to ARL, MRL is a better performance criterion to use. It is demonstrated that the claims for its superior performance over the synthetic  $np$  and DS  $np$  charts are based on the fact that ZS mode has a hidden feature that gives it a head-start. However, for the majority of SPC applications, it is more crucial to assess the control chart's statistical performance after a prolonged time of IC operation (i.e., when the process is in SS mode), when it is necessary to detect a shift in the process. It has been discussed how to employ the Markov chain to perform MRL SS analyses for the SDS chart for attribute data. This method has been used to compare the SDS  $np$  chart with the synthetic  $np$  and the DS  $np$  charts for a wide range of cases. These comparisons adequately demonstrate that the performance of the SDS  $np$  chart does not significantly outperform the DS  $np$  chart. Overall, the SDS  $np$  chart outperforms the DS  $np$  chart when  $\gamma_{\text{opt}} = 1.5$  and  $np_0 = 0.5$  for different combinations of  $(n, p_0) = (100, 0.005)$  and  $(50, 0.01)$ . Note that the optimization designs based on minimizing the EMRL offer the practitioners with the optimal parameter for the chart which performs favourably for a range of shift sizes, i.e., from the lower to upper range of shift sizes when the actual shift size is unknown in advance. In short, the optimal charting parameters reported in this study are helpful to quality practitioners since these results enable the SDS  $np$  chart to be implemented quickly.

**Author Contributions:** M.H.T., conceptualization, methodology, software, formal analysis, investigation, data curation, project administration, writing—original draft. C.M.L.K. and H.S.C.; software, validation, resources, writing—review and editing. M.F.L. and Y.H.R.C.; validation, visualization, writing—review and editing. All authors have read and agreed to the published version of the manuscript.

**Funding:** This research received no external funding.

**Institutional Review Board Statement:** Not applicable.

**Informed Consent Statement:** Not applicable.

**Data Availability Statement:** The data that support the findings of this study are available from the corresponding author, upon reasonable request.

**Acknowledgments:** Immense recognition is rendered to all Computational Laboratory personnel for their support and constructive input.

**Conflicts of Interest:** The authors declare no conflict of interest.

## References

1. Khoo, M.B.C.; Lee, H.C.; Wu, Z.; Chen, C.H.; Castagliola, P. A synthetic double sampling control chart for the process mean. *IIE Trans.* **2010**, *43*, 23–38. [\[CrossRef\]](#)
2. Khoo, M.B.C.; Wu, Z.; Castagliola, P.; Lee, H.C. A multivariate synthetic double sampling  $T^2$  control chart. *Comput. Ind. Eng.* **2013**, *64*, 179–189. [\[CrossRef\]](#)
3. Bourke, P.D. Detecting a shift in fraction nonconforming using run-length control charts with 100% inspection. *J. Qual. Technol.* **1991**, *23*, 225–238. [\[CrossRef\]](#)
4. Lee, M.H.; Khoo, M.B.C. Synthetic double sampling s chart. *Commun. Stat.-Theory Methods* **2017**, *46*, 5914–5931. [\[CrossRef\]](#)
5. Costa, A.F.B.; Machado, M.A.G. The steady-state behavior of the synthetic and side-sensitive synthetic double sampling charts. *Qual. Reliab. Eng. Int.* **2015**, *31*, 297–303. [\[CrossRef\]](#)
6. Haq, A.; Khoo, M.B.C. A synthetic double sampling control chart for process mean using auxiliary information. *Qual. Reliab. Eng. Int.* **2019**, *35*, 1803–1825. [\[CrossRef\]](#)
7. You, H.W.; Khoo, M.B.C.; Lee, M.H.; Castagliola, P. Synthetic double sampling  $\bar{X}$  chart with estimated process parameters. *Qual. Technol. Quant. Manag.* **2015**, *12*, 579–604. [\[CrossRef\]](#)
8. You, H.W. Performance of synthetic double sampling chart with estimated parameters based on expected average run length. *J. Probab. Stat.* **2018**, *2018*, 7583610. [\[CrossRef\]](#)
9. Lorenzen, T.J.; Vance, L.C. The economic design of control charts: A unified approach. *Technometrics* **1986**, *28*, 3–10. [\[CrossRef\]](#)
10. Lee, M.H.; Khoo, M.B.C. Economic-statistical design of synthetic double sampling  $T^2$  chart. *Commun. Stat.-Theory Methods* **2019**, *48*, 5862–5876. [\[CrossRef\]](#)
11. Lee, M.H.; Khoo, M.B.C. The economic and economic statistical designs of synthetic double sampling  $\bar{X}$  chart. *Commun. Stat.-Simul. Comput.* **2019**, *48*, 2313–2332. [\[CrossRef\]](#)
12. Aghaolur, C.D.; Ezekwem, C. An economic design of a modified synthetic double sampling control chart for process monitoring. *Int. J. Eng. Res. Technol.* **2016**, *5*, 445–460.
13. Chong, Z.L.; Khoo, M.B.C.; Castagliola, P. Synthetic double sampling np control chart for attributes. *Comput. Ind. Eng.* **2014**, *75*, 157–169. [\[CrossRef\]](#)
14. Tuh, M.H.; Kon, C.M.L.; Chua, H.S.; Lau, M.F.; Chang, R.Y.H. A study of synthetic double sampling np chart based on median run length. In Proceedings of the 2022 3rd International Conference on Artificial Intelligence and Data Sciences (AiDAS), Ipoh, Malaysia, 7–8 September 2022.
15. Knoth, S. The case against the use of synthetic control charts. *J. Qual. Technol.* **2016**, *48*, 178–195. [\[CrossRef\]](#)
16. Malela-Majika, J.C. Modified side-sensitive synthetic double sampling monitoring scheme for simultaneously monitoring the process mean and variability. *Comput. Ind. Eng.* **2019**, *130*, 798–814. [\[CrossRef\]](#)
17. Davis, R.B.; Woodall, W.H. Evaluating and improving the synthetic control chart. *J. Qual. Technol.* **2002**, *34*, 200–208. [\[CrossRef\]](#)
18. Bourke, P.D. Performance comparisons for the synthetic control chart for detecting increases in fraction nonconforming. *J. Qual. Technol.* **2008**, *40*, 461–475. [\[CrossRef\]](#)
19. Teoh, W.L.; Khoo, M.B.C.; Castagliola, P.; Chakraborti, S. Optimal design of the double sampling  $\bar{X}$  chart with estimated parameters based on median run length. *Comput. Ind. Eng.* **2014**, *67*, 104–115. [\[CrossRef\]](#)
20. Khoo, M.B.C.; Wong, V.H.; Wu, Z.; Castagliola, P. Optimal design of the synthetic chart for the process mean based on median run length. *IIE Trans.* **2012**, *44*, 765–779. [\[CrossRef\]](#)
21. Lee, M.H.; Khoo, M.B.C. Optimal designs of multivariate synthetic  $|S|$  control chart based on median run length. *Commun. Stat.-Theory Methods* **2017**, *46*, 3034–3053. [\[CrossRef\]](#)
22. Graham, M.A.; Chakraborti, S.; Mukherjee, A. Design and implementation of CUSUM exceedance control charts for unknown location. *Int. J. Prod. Res.* **2014**, *52*, 5546–5564. [\[CrossRef\]](#)
23. Chakraborti, S. Run length distribution and percentiles: The Shewhart chart with unknown parameters. *Qual. Eng.* **2007**, *19*, 119–127. [\[CrossRef\]](#)
24. Teoh, W.L.; Chong, J.K.; Khoo, M.B.C.; Castagliola, P.; Yeong, W.C. Optimal designs of the variable sample size chart based on median run length and expected median run length. *Qual. Reliab. Eng. Int.* **2017**, *33*, 121–134. [\[CrossRef\]](#)
25. Tang, A.; Castagliola, P.; Sun, J.; Hu, X. Optimal design of the adaptive EWMA chart for the mean based on median run length and expected median run length. *Qual. Technol. Quant. Manag.* **2019**, *16*, 439–458. [\[CrossRef\]](#)
26. Qiao, Y.; Sun, J.; Castagliola, P.; Hu, X. Optimal design of one-sided exponential EWMA charts based on median run length and expected median run length. *Commun. Stat.-Theory Methods* **2022**, *51*, 2887–2907. [\[CrossRef\]](#)
27. Chong, Z.L.; Tan, K.L.; Khoo, M.B.C.; Teoh, W.L.; Castagliola, P. Optimal designs of the exponentially weighted moving average (EWMA) median chart for known and estimated parameters based on median run length. *Commun. Stat.-Simul. Comput.* **2022**, *51*, 3660–3684. [\[CrossRef\]](#)

28. Tuh, M.H.; Kon, C.M.L.; Chua, H.S.; Lau, M.F. Optimal Statistical Design of the Double Sampling np chart based on Expected Median Run Length. *Front. Appl. Math. Stat.* **2022**, *8*, 993152. [[CrossRef](#)]
29. De Araujo Rodrigues, A.A.; Epprecht, E.K.; De Magalhaes, M.S. Double-sampling control charts for attributes. *J. Appl. Stat.* **2011**, *38*, 87–112. [[CrossRef](#)]
30. Tuh, M.H.; Lee, M.H.; Lau, M.F.; Then, P.H.H. Performance of the double sampling np chart based on the median run length. *Adv. Math. Sci. J.* **2020**, *9*, 7429–7438. [[CrossRef](#)]
31. Brook, D.; Evans, D.A. An approach to the probability distribution of CUSUM run length. *Biometrika* **1972**, *59*, 539–549. [[CrossRef](#)]
32. Champ, C.W. Steady-state run length analysis of a Shewhart quality control chart with supplementary runs rules. *Commun. Stat.-Theory Methods* **1992**, *21*, 765–777. [[CrossRef](#)]
33. Gan, F.F. The run length distribution of a cumulative sum control chart. *J. Qual. Technol.* **1993**, *25*, 205–207. [[CrossRef](#)]
34. You, H.W.; Khoo, M.B.C.; Castagliola, P.; Qu, L. Optimal exponentially weighted moving average charts with estimated parameters based on median run length and expected median run length. *Int. J. Prod. Res.* **2016**, *54*, 5073–5094. [[CrossRef](#)]
35. Castagliola, P.; Celano, G.; Psarakis, S. Monitoring the coefficient of variation using EWMA charts. *J. Qual. Technol.* **2011**, *43*, 249–265. [[CrossRef](#)]
36. Winckel, G.; Legendre-Gauss Quadrature Weights and Nodes. MATLAB Central File Exchange 2022. Available online: <https://www.mathworks.com/matlabcentral/fileexchange/4540-legendre-gauss-quadrature-weights-and-nodes> (accessed on 5 January 2022).
37. Lee, M.H.; Khoo, M.B.C. Optimal design of synthetic np control chart based on median run length. *Commun. Stat.-Theory Methods* **2017**, *46*, 8544–8556. [[CrossRef](#)]
38. Tang, A.; Castagliola, P.; Sun, J.; Hu, X. The effect of measurement errors on the adaptive EWMA chart. *Qual. Reliab. Eng. Int.* **2018**, *34*, 609–630. [[CrossRef](#)]
39. Oakland, J.S. *Statistical Process Control*, 6th ed.; Routledge: New York, NY, USA, 2007.

**Disclaimer/Publisher's Note:** The statements, opinions and data contained in all publications are solely those of the individual author(s) and contributor(s) and not of MDPI and/or the editor(s). MDPI and/or the editor(s) disclaim responsibility for any injury to people or property resulting from any ideas, methods, instructions or products referred to in the content.